PA28γ–20S proteasome is a proteolytic complex committed to degrade unfolded proteins

Jean-Yves Alejandro Frayssinhes1, Fulvia Cerruti1, Justine Laulin2, Angela Cattaneo3, Angela Bachi4, Sebastien Apcher2, Olivier Coux5 and Paolo Cascio1,*

1 Department of Veterinary Sciences, University of Turin, Largo P. Braccini 2, 10095, Grugliasco, Turin, Italy

2 Université Paris-Saclay, Institut Gustave Roussy, Inserm, Immunologie des tumeurs et Immunothérapie, Villejuif, France.

3 Cogentech SRL Benefit Corporation, 20139 Milan, Italy

4 The FIRC Institute of Molecular Oncology (IFOM), 20139 Milan, Italy

5 Centre de Recherche de Biologie cellulaire de Montpellier (CRBM), CNRS UMR 5237, Université de Montpellier, 1919 Route de Mende, 34293, Montpellier, France

PA28γ-20S proteasome is a proteolytic complex committed to degrade unfolded proteins

Cellular and Molecular Life Sciences

Published on-line 16 December 2021

Pag. 1-15

DOI 10.1007/s00018-021-04045-9

PA28γ-20S proteasome is a proteolytic complex committed to degrade unfolded proteins

Jean-Yves Alejandro Frayssinhes[1], Fulvia Cerruti[1], Justine Laulin[2], Angela Cattaneo[3], Angela Bachi[4], Sebastien Apcher[2], Olivier Coux[5] and Paolo Cascio[1,*]

[1] Department of Veterinary Sciences, University of Turin, Largo P. Braccini 2, 10095, Grugliasco, Turin, Italy

[2] Université Paris-Saclay, Institut Gustave Roussy, Inserm, Immunologie des tumeurs et Immunothérapie, Villejuif, France.

[3] Cogentech SRL Benefit Corporation, 20139 Milan, Italy

[4] The FIRC Institute of Molecular Oncology (IFOM), 20139 Milan, Italy

[5] Centre de Recherche de Biologie cellulaire de Montpellier (CRBM), CNRS UMR 5237, Université de Montpellier, 1919 Route de Mende, 34293, Montpellier, France

***** Correspondence: paolo.cascio@unito.it

Acknowledgments: We thank Francesco Turci and Francesco Ferrini for help in preparing figures, Patrick Moore for assistance in preparation of the manuscript and Massimo Coletta for insightful discussions

Abstract

PA28γ is a nuclear activator of the 20S proteasome that, unlike the 19S regulatory particle, stimulates hydrolysis of several substrates in an ATP- and ubiquitin-independent manner and whose exact biological functions and molecular mechanism of action still remain elusive. In an effort to shed light on these important issues, we investigated the stimulatory effect of PA28γ on the hydrolysis of different fluorogenic peptides and folded or denatured full-length proteins by the 20S proteasome. Importantly, PA28γ was found to dramatically enhance breakdown rates by 20S proteasomes of several naturally or artificially unstructured proteins, but not of their native, folded counterparts. Furthermore, these data were corroborated by *in cellulo* experiments with a nucleus-tagged myelin basic protein. Finally, mass spectrometry analysis of the products generated during proteasomal degradation of two proteins demonstrated that PA28γ does not increase, but rather decreases, the variability of peptides that are potentially suitable for MHC class I antigen presentation. These unexpected findings indicate that global stimulation of the hydrolysis of unfolded proteins may represent a more general feature of PA28γ and suggests that this proteasomal activator might play a broader role in the pathway of protein degradation than previously believed.

Keywords: PA28γ; proteasome; proteasome activator; proteasome gate; protein degradation; ATP-independent proteolysis

Declarations

Funding: Ricerca Locale (ex 60%) to P.C.

Conflicts of interest/Competing interests: The authors declare no conflict of interest

Availability of data and material: MS data as raw files, peptides identified with relative intensities and search parameters have been deposited to the ProteomeXchange Consortium via the PRIDE partner repository with the dataset identifier PXD029248.

Code availability: Not applicable

Author Contributions: Jean-Yves Alejandro Frayssinhes**,** Acquisition, analysis and interpretation of data; Fulvia Cerruti, Acquisition, analysis and interpretation of data; Justine Laulin, Acquisition, analysis and interpretation of data; Angela Cattaneo, Acquisition, analysis and interpretation of data, Angela Bachi, Analysis and interpretation of data Apcher Sebastien, Analysis and interpretation of data; Olivier Coux, Analysis and interpretation of data; Paolo Cascio, Conception and design, Acquisition of data, Analysis and interpretation of data, Drafting the article.

Introduction

The vast majority of intracellular proteins in eukaryotic cells are hydrolyzed by the 26S proteasome, a large (2.4 MDa) multimeric protease abundantly expressed in the nucleus and cytosol [1]. The 26S proteasome is composed of the 20S core particle, which in its internal cavity harbors the proteolytic sites and the 19S regulatory particle, which used for recognition, unfolding, and translocation of protein substrates within the protease [2]. The 20S proteasome is the central core of this proteolytic macromolecular machine, has a cylindrical structure with a molecular weight of ~700 kDa, and is formed by four overlapping rings of seven subunits each. The two outer rings are constituted of α subunits, and the two inner ones of β subunits [3]. The catalytic active sites of the constitutive 20S proteasomes are located on the β1, β2, and β5 subunits. However, under the stimulus of γ-interferon or other pro-inflammatory cytokines, new catalytic subunits are synthesized (β1i, β2i, and β5i) which replace those constitutive in so-called newly assembled 20S immunoproteasomes, which are optimized to generate the antigenic peptides (or epitopes) that are presented on the cell surface in association with MHC class I complexes [4]. In general, proteasomes can cleave any peptide bond except those at the C-terminus of proline; peptidase activities defined by fluorogenic substrates recognize three cleavage specificities: trypsin-like (i.e. hydrolysis after basic residues), chymotrypsin-like (i.e. hydrolysis after hydrophobic residues,), and caspase-like (i.e. after acidic residues) [5].

Another important family of 20S proteasome regulators is that of the ATP- and ubiquitin-independent PA28 activators (also called 11S, REG or PMSE), which in vertebrates is formed by three highly homologous subunits α, β, and γ [6]. The crystal structure of PA26 (a homologue of PA28 in *Trypanosoma brucei*) clearly reveals that binding with the activator determines the opening of the gate, formed by the N-terminal tails of the α subunits, which normally occludes the access to (and exit from) the internal proteolytic cavity [7]. It is generally assumed that this represents the main molecular mechanism of action of all the other members of this class of proteasome activators [8]. Accordingly, opening of the gate, although with a related but different molecular mechanism, has also been described for a PA28 homolog present in *Plasmodium falciparum*, whose structure in association with the homospecific 20S particle has recently been solved. Interestingly, in this case PA28 was found to bind 20S asymmetrically, strongly engaging subunits on only one side of the core particle [9]. However, strong evidence indicating that PA28 may also act through long distance allosteric modifications of proteasomal proteolytic sites has been recently reported [10-12].

PA28 α and β form a heteroheptameric ring with a subunit stoichiometry of 4α3β [13] present in both the nucleus and cytosol of mammalian cells and whose formation is highly induced by γ-interferon [14]. PA28αβ *in vitro* strongly stimulates hydrolysis of short peptides by all three peptidase activities of 20S proteasomes, but not of full-length proteins, regardless of whether they are ubiquitinated, properly folded, or completely denatured [15-18]. However, a specific

function of PA28αβ, predominantly in association with the immunoproteasome in promoting the degradation of oxidized proteins, has been also described, which may indicate that it plays a role in adaptive responses to stressful conditions [19-24]. *In vivo* PA28αβ exerts a clear action of stimulation of MHC class I antigen presentation, although this activity is restricted to only some epitopes [25]. On the contrary, PA28γ forms homoheptameric rings that are located exclusively in the nucleus and which are not induced (and even reduced) by γ-interferon [26]. PA28γ was initially reported to exclusively enhance the trypsin-like activity of proteasomes [27, 28], but additional data indicates that it can also stimulate the other two (i.e. chymotrypsin- and caspase-like) peptidase activities [29-31]. Importantly, PA28γ was shown to increase degradation of some full-length proteins through both direct and indirect mechanisms [32]. Specifically, the list of proteins that are directly targeted by PA28γ towards proteasomal degradation in an ATP- and ubiquitin-independent process includes the oncogenic proteins steroid receptor coactivator SRC-3 [33], HCV core protein [34], pituitary tumor-transforming 1 PTTG1 [35], cyclin-dependent kinase inhibitors p21 [36], p16, and p19 [37]. PA28γ has also been shown to strongly reduce the stability of the tumor suppressor p53 through an indirect mechanism of stimulus involving ubiquitination by the ubiquitin-ligase MDM2 and subsequent ubiquitin- and ATP-dependent 26S proteasome degradation [38]. The exact biological functions of PA28γ have not yet been fully elucidated, although this proteasome activator is clearly involved in the regulation of several essential cellular pathways, including cell growth and proliferation [39], transition from G to S phase in the cell cycle [40], inhibition of apoptosis [41], chromosomal stability [42], nuclear dynamics through modulation of the number and size of various nuclear bodies, including Cajal bodies (CBs) [43], nuclear speckles [43], promyelocytic leukemia protein bodies [44], cellular response to DNA double-strand breaks [45], autophagy inhibition [46], spermatogenesis [31], neoplastic transformation [47-49] , and MCH class I antigen presentation [50, 51]. Since in previous studies we demonstrated that heteroheptameric PA28αβ profoundly modifies the size and composition of amino acid sequences of products generated during proteasomal degradation of unfolded proteins without, however, affecting the overall rates of substrate hydrolysis [18], the present study was undertaken to determine whether similar biochemical behavior is also shared by the homolog PA28γ.

Materials and Methods

Proteins purification

Recombinant PA28γ and PA28αβ was expressed in *E. coli* and purified as described previously [30, 52]. Human 20S proteasome was purified from extracts of HeLa cells (Ipracell, Mons, BE) using classic chromatographic procedures as reported [30]. All preparations were free of contaminant endo- and exo-proteolytic activities that may interfere with proteasomal degradation experiments. PA28γ- and PA28αβ-20S proteasomes were reconstituted by preincubating 20S particles with a 6-fold molar excess of PA28γ at 37°C for 30 min in 20 mM HEPES, pH 7.5, and were used immediately for degradation experiments.

Peptidase assays and kinetic analysis

Peptidase activities of 20S proteasomes were measured using specific fluorogenic substrates (Bachem, Bubendorf, CH) at concentrations between 100 and 200 μM in 20 mM Tris–HCl pH 7.5, 0.2% BSA as previously described [53]. Briefly, the fluorescence of released amc (excitation, 380 nm; emission, 460 nm) was monitored continuously at 37°C with a Carry Eclipse spectrofluorometer (VARIAN, Palo Alto, CA, USA). Assays were calibrated using standard solutions of the free fluorophore, and reaction velocities were calculated from the slopes of the initial linear portions of the curves. Substrate consumption at the end of incubation never exceeded 1%. Kinetic parameters of the PA28γ-20S complexes were calculated by assessing reaction velocities at different activator concentrations. The best-fit was performed using GraphPad prism (version 5) software through nonlinear-regression for enzyme kinetics.

Protein degradation and analysis of peptide products

Degradation of β-casein, IGF-1, MBP and α-lactalbumin were performed as previously described [18, 54]. Reduction and carboxymethylation of IGF-1 and α-lactalbumin to ensure denaturation and prevent sulfhydryl bond formation were performed according to published methods [55]. To study the kinetics of substrate degradation using fluorescamine, casein (710 μM), IGF-1 (830 μM), MBP (85 μM), and α-lactalbumin (307 μM) were incubated with 20S and PA28γ-20S proteasomes (20 to 80 nM depending on the substrate) in 20 mM HEPES, pH 7.5. Epoxomicin (Enzo Life Sciences, Farmingdale, New York) was used at a final concentration of 20 μM. To assay peptides generated during protein degradation, at the indicated time points peptide products were separated from undegraded protein by ultrafiltration through a membrane with a 3 kDa cut-off (Pall Corporation, NY, USA), and the appearance of new amino groups was measured using fluorescamine [55]. Consumption of the substrate at the end of the 8-hr incubation never exceeded 10%. Degradation of IGF-1 (400 μM), MBP (90 μM), and α-lactalbumin (260 μM) by 20S and PA28-20S

proteasomes (120 nM for IGF-1 and α-lactalbumin, 5.6 nM for MBP) for electrophoretic analysis was performed at 37°C in the same buffer described previously. At 0, 4, 8 and 12 h aliquots were taken, the undegraded protein was separated on a 12% (for MBP) or 18% (for IGF-1) SDS-PAGE gel, and densitometric analysis of Coomassie-stained bands was performed with a VersaDoc 1000 Imaging System (Bio-Rad Laboratories, Hercules, CA, USA) using Quantity One software (Bio-Rad Laboratories, Hercules, CA, USA). For HP-size exclusion chromatography of β-casein products, peptides generated during an 8 hr hydrolysis reaction were isolated by ultrafiltration using both 3 and 10 kDa cut-off membranes (Pall Corporation, NY, USA), which gave very similar results in terms of size distribution of proteasome products. After that, equal amounts of peptides were diluted in 0.1 M HEPES, pH 6.8, and separated on a polyhydroxy-ethyl aspartamide column (0.46 x 20 cm, Poly LC, Columbia, MD, USA) using an HP1100 HPLC (Hewlett-Packard, Palo Alto, CA, USA) equipped with a fluorometer. The mobile phase was 0.2 M Na_2SO_4, 25% acetonitrile (pH 3.0; adjusted with phosphoric acid) at a flow rate of 0.125 ml/min. For each analysis, 20 µl of peptide solution was added to 16 µl of fluorescamine (dissolved 0.3 mg/ml in acetonitrile). The reaction was terminated after 30 sec with 22 µl of H_2O, and the sample was immediately injected on the HPLC column. The fluorescence of eluted material was monitored continuously and a blank run (corresponding to time 0 hr of the degradation reaction) was always subtracted. To determine the apparent molecular mass of peptides eluted, the column was calibrated with 19 standard amino acids and peptides in the 75-3500 Da range that had been derivatized with fluorescamine in the same manner as proteasomal degradation products. Prior control studies showed that retention times of these fluorescamine-derivatized products are highly reproducible and linearly dependent on the logarithm of their molecular weights, and that recovery of amino acids and peptides of different lengths is quantitative [18]. Note that amino acids and peptides eluting from the column are bound to fluorescamine, whose molecular weight must be subtracted to calculate the actual mass of proteasomal products. Mean and median sizes of peptides generated by 20S and PA28γ-20S proteasomes were calculated from the distributions of products obtained by SEC, assuming an average molecular weight of 110 Da for each residue.

Liquid chromatography–tandem MS (LC–MS/MS) analysis

Samples from the 20S -/+ PA28γ 6 hour degradation experiments containing approximately 5 (for IGF-1) and 30 (for MBP) pmol NH_2/µl were loaded onto a StageTipsµC18 column [56]; peptides were eluted in 40 µl 80% acetonitrile in 0.1% formic acid. The acetonitrile was allowed to evaporate in a Speed-Vac, and samples were then resuspended in 10 µl of eluent A (see composition below) for nLC-MS/MS analysis. Two microliters of each sample were injected as technical replicates into a nLC–ESI–MS/MS quadrupole Orbitrap QExactive-HF mass spectrometer (Thermo Fisher Scientific). Peptide separation was achieved using a linear gradient from 95% solvent A (2% ACN, 0.1% formic acid) to

50% solvent B (80% acetonitrile, 0.1% formic acid) for 23 min and from 60 to 100% solvent B for 2 min at a constant flow rate of 0.25 µl/min on a UHPLC Easy-nLC 1200 (Thermo Scientific) connected to a 25-cm fused-silica emitter with an inner diameter of 75 µm (New Objective, Inc. Woburn, MA, USA), packed in-house with ReproSil-Pur C18-AQ 1.9-µm beads (Dr. Maisch Gmbh, Ammerbuch, Germany) using a high-pressure bomb loader (Proxeon, Odense, Denmark). MS data were acquired using a data-dependent top-15 method for HCD fragmentation. Survey full-scan MS spectra (300–1750 Th) were acquired in the Orbitrap at a resolution of 60,000, an AGC target of $1x10^{e6}$, and an IT of 120 ms. For HCD spectra, the resolution was set to 15,000 at *m*/*z* 200, with an AGC target of 1^{e5}, an IT of 120 ms, an NCE of 28% and an isolation width of 3.0 *m*/*z*.

Data processing and analysis

For quantitative proteomics analysis, raw data were processed with MaxQuant (ver. 1.6.0.16) and searched against a database containing the sequence of the IGF-1 and MBP + contaminant fasta included in MaxQuant. No enzyme specificity was selected, and there were no differences between I and L. The mass deviation for MS/MS peaks was set at 20 ppm, and the peptide false discovery rate (FDR) was set at 0.01. The list of identified peptides was filtered to eliminate contaminants. Statistical analyses were performed with Perseus (ver. 1.6.2.3) considering the peptide intensity; normalization based on the Z-score and imputation was applied. Significant peptides were determined with a t-test, Benjamini Hochberg correction, and FDR<0.05. Only significant peptides were used for supervised hierarchical clustering analysis. MS data as raw files, peptides identified with relative intensities and search parameters have been deposited to the ProteomeXchange Consortium via the PRIDE [57] partner repository with the dataset identifier PXD029248.

MBP expression *in cellulo*

The gene coding for MBP isoform (transcript variant 1) containing in its sequence a nontraditional PY-Nuclear Localization Signal (NLS) was purchased from Origene and insert in pCMV6-Entry eukaryotic expression plasmid. The A375 (ATCC, nCRL-1619) human melanoma cells and the derivative clone A375 Crispr knockout for PA28γ have been described in detail [51] and were cultured according to ATCC's protocol. Once a month, mycoplasma contamination in cell cultures was assessed using the Venor®GeM OneStep mycoplasma detection kit (Minerva biolabs). Cells were used within four weeks after thawing (~10 passages) and were transfected with 1 µg of plasmid DNA along with 2 µl of JetPrime according to the manufacturer's protocol (Ozyme). Importantly, no difference in growth rates was observed between WT A375 and A375 Crispr cells. For Western Blots, cells were lysed in RIPA buffer supplemented with

Complete™ Protease Inhibitor (Roche, #11697498001) and centrifuged at 16 000xg for 20 min at 4°C. Protein concentration of the supernatant was determined by BCA-assay using the Pierce™ BCA Protein Assay Kit (Thermo Fisher Scientific). 15 µg of proteins were denatured for 10 min at 95°C in 1X Laemmli Sample Buffer containing 2.5% β-mercaptoethanol. Proteins were loaded on 4-15% acrylamide gels and run at 100 V in 1X TGS Buffer. Proteins were then transferred onto PVDF membranes using a Trans-Blot Semi-Dry Transfer Cell (Bio-Rad). Membranes were blocked for 1 hour with 5% milk solution and incubated with primary antibody overnight at 4°C. The day after the blot was incubated with a secondary antibody coupled with HRP for 1h at RT. An anti-β-actin antibody (Santa Cruz, #sc47778) coupled with HRP was used as a loading control. Depending on the experiment, the following primary and secondary antibodies were used: anti-Myc-tag (9B11) mouse mAb (Cell Signaling, #2276), anti-PA28γ recombinant rabbit mAb (Thermo Fisher Scientific, #700180), anti-p21 Waf1/Cip1 (12D1) rabbit mAb (Cell Signaling, #2947), anti-β-actin antibody coupled with HRP (Santa Cruz, #sc47778), polyclonal swine anti-rabbit immunoglobulins/HRP (Dako, #P0217) and polyclonal rabbit anti-mouse immunoglobulins/HRP (Dako, #P0260).

Statistical analyses

To compare average measurements of generation of amino group and protein degradation and expression levels, we adopted a non-parametric Mann-Whitney test.

Results

PA28γ differently affects 20S proteasome peptidase activities

In a preliminary effort aimed at better characterizing the exact biochemical properties of PA28γ activator, we assessed its effects on the hydrolysis of a panel of short fluorogenic peptides specifically designed to probe endopeptidase activities. To perform these (and the following) experiments, we utilized a recombinant protein expressed in *E. coli* and purified to homogeneity as described in the Materials and Methods. Importantly, size exclusion chromatography of the final preparation demonstrated complete conversion of the PA28γ monomer into a stable high molecular weight complex of apparent MW of ~200 kDa, consistent with that of a heptameric ring (Supplementary Figure 1A). Initially, we showed that of the 12 fluorogenic peptides tested (four designed to probe chymotrypsin-like, CT-L, two caspase-like, C-L, and six trypsin-like T-L, endopeptidase activities), all were cleaved by human 20S particles although at greatly divergent rates, as expected for substrates that differ in both length and amino acid composition (Supplementary Table 1). Next, we investigated the effect of increasing concentrations of PA28γ on degradation rates of these proteasomal substrates. As shown in Supplementary Figure 2, a strong dose-dependent acceleration of the rate of hydrolysis reactions could be observed for 10 peptides, and this stimulation involved substrates cleaved by all three proteasome active sites. Consequently, the maximal specific activity of 20S particles completely activated by PA28γ (i.e. 20S bound at both side with a PA28γ ring) varied from ~2 to ~450 nmol of peptide cleaved per min/mg of enzyme depending on the substrate (Table 1). Interestingly, however, the extent of this PA28γ-dependent stimulation (compared to the basal activity of 20S in absence of the activator) was not constant, but ranged between 4- and 18-fold, and unexpectedly differed strongly even between peptides cleaved by the same proteasomal active site (Table 1). Furthermore, careful analysis of the mechanism of 20S activation with increasing amounts of PA28γ showed a kinetic trend consistent with a rectangular hyperbola, with a concentration of the activator in the nanomolar range required to fully activate picomolar concentrations of proteasome (Supplementary Figure 2). Of note, the non-sigmoid shape of the activation kinetics of hydrolysis of the fluorogenic peptide indicates the absence of cooperative binding between the two PA28γ molecules that associate with the two opposite ends of the 20S particle. In contrast with these results, hydrolysis by proteasomal trypsin-like activity of two dipeptides (LR and FR), unlike that of a third one which is very similar (RR), was completely unaffected by the presence of high concentrations of PA28γ (Supplemetary Figure 3A). Of note this took place when all three peptides were tested at a concentration (i.e. 100 μM) at which the catalytic sites of the 20S are not saturated by the substrate, and therefore below Vmax (Supplementary Figure 3B).

PA28γ enhances rates of peptide bond cleavage in the full-length protein β-casein

If on the one hand short fluorogenic peptides represent useful tools to investigate the biochemical properties of proteasomal peptidase sites, on the other hand their hydrolysis only roughly mirrors the complex process of degradation of real, physiological substrates of proteasomes, which *in vivo* mainly degrade proteins rather than short polypeptides [58, 59]. For this reason, we decided to investigate the effect of PA28γ on degradation of full-length proteins. To this end, we initially chose β-casein, widely used for biochemical studies as a proteasome substrate, which has little tertiary structure and thus does not require artificial denaturation to be degraded at detectable rates by 20S particles [55, 60-63]. As shown in Figure 1A, the rates of appearance of new amino groups, generated as a consequence of the hydrolysis of peptide bonds in the protein and assessed by means of fluorescamine, were linear for up to 8 hr for both proteasome species analyzed (i.e. 20S and PA28γ-20S). Moreover, as demonstration of the absolute dependence on the proteasome of the hydrolysis reaction, NH_2 generation was completely absent in the presence of the more specific proteasome inhibitor epoxomicin (Figure 1A) and when the substrate was incubated alone or with only PA28γ (Supplementary Figure 4A and B). More importantly, however, the PA28γ-20S particles reproducibly released 3-fold more NH_2 at each time point than unligated 20S (Figure 1A). This finding was surprising because PA28γ has generally been reported to be able to stimulate proteasomal degradation of small peptides, but only very few full-length proteins [32, 64] and, to the best of our knowledge, not for β-casein.

Association of PA28γ with 20S does not affect size distribution of products generated during hydrolysis of casein

Theoretically, the higher rate of generation of primary amino groups by PA28γ-20S proteasomes might be caused by either enhanced substrate hydrolysis induced by the activator or, alternatively, by a significant reduction of size distribution of peptide products generated (i.e., even in the absence of modifications in the rates of β-casein consumption), as in the case of the homolog PA28αβ [18]. To discriminate between these two alternatives, we analyzed the size distribution of products generated during hydrolysis of casein by 20S and PA28γ-20S particles using an HP-size exclusion chromatographic method that allows linear separation and accurate quantification of peptides in the range of 1 to 30 residues (Supplementary Figure 5).

In particular, the protein was degraded at linear rates and under conditions ensuring that peptides released by proteasomes do not re-enter the degradative particle, and therefore not subjected to a second round of hydrolysis (i.e. the substrate was present in large excess and not more than 10% was degraded at the end of the incubation) [54]. When analyzed by this approach, peptides generated from casein by the 20S and PA28γ-20S proteasomes were found to fall into a continuum of size distribution ranging from 1 to 30 residues (Figure 1B) that appeared to fit a lognormal distribution, which is in agreement with previous analyses of different substrates and proteasome species [61, 63, 65].

Specifically, the chromatographic profile of 20S proteasome products was characterized by a large peak that culminates at the size of 2-3 residues with a small shoulder corresponding to less than 3% of the total fluorescence signal eluting from the column) in correspondence of sizes between 30 to 16 residues (Figure 1B). Of interest, a nearly superimposable profile was also detected for peptides generated by PA28γ-20S particles (Figure 1B). In this case, the only minor differences in size distribution involved a reduction of about two-thirds in the minor peak of larger (>16) residues accompanied by a small, but reproducible, shift towards a high molecular weight of the peak of the main products when PA28γ associated with 20S particles (Figure 1B). Moreover, if samples fractionated by SEC-HPLC were not normalized by the amount of peptides generated, but equal volumes of degradation reaction carried out with equimolar amounts of enzymes (i.e. 20S and PA28γ-20S proteasomes) were analyzed, the profile of the peak of PA28γ-20S products did not change. This is in good agreement with the kinetic data shown in Figure 1A, and its height and area are increased about 3-fold (data not shown). As a result, the means of product lengths calculated from HPLC size distributions were the same (4 residues) for 20S and PA28γ-20S proteasomes and the medians (~3 residues) were also very similar (Figure 1C).

PA28γ but not PA28αβ consistently stimulates hydrolysis of different unfolded proteins by the 20S proteasome

To assess whether the unexpected finding that PA28γ is able to promote proteasomal degradation of the naturally disordered substrate β-casein might imply a more general, and so far unrecognized, property of this activator, we challenged its role in degradation of several unrelated, unfolded proteins by the 20S particle. To this end we utilized another natively unfolded substrate, myelin basic protein (MBP), and two chemically denatured proteins, insulin-like growth factor 1 (IGF-1) and α-lactalbumin. As shown in Figure 2, the rates of peptide bond cleavage by the 20S proteasome were dramatically enhanced for all three substrates in the presence of PA28γ. Furthermore, as for β-casein, the dependence on the proteasome of the hydrolysis reaction was demonstrated by the absence of NH_2 generation in the presence of epoxomicin (Figure 2) or when the substrates were incubated alone or only with PA28γ (Supplementary Figure 6). Moreover, the absolute specificity for unfolded proteins of the PA28γ-induced proteolytic stimulation was unambiguously shown by directly comparing the rates of proteasomal hydrolysis of chemically unfolded IGF-1 and α-lactalbumin with those of their native, folded counterparts. In fact, rates of proteasomal hydrolysis of folded IGF-1 and α-lactalbumin were nearly undetectable (data not shown) and only minimally affected by the presence of PA28γ, in striking contrast with what observed for their corresponding denatured forms (Figure 3).

Further direct and unequivocal evidence of the enhancement of proteins turnover rates induced by PA28γ was subsequently obtained by following the disappearance of undigested substrates incubated for several hours in the presence

of 20S proteasome alone or conjugated with PA28γ. These experiments clearly demonstrated that the presence of PA28γ strongly accelerates the kinetics of full-length unfolded proteins hydrolysis by the 20S proteasome (Figure 4). This result appears even more remarkable in light of the fact that, in parallel experiments, PA28αβ was unable to activate denatured protein degradation (Figure 4), in accordance with what has already been published for other full length substrates [15, 16, 18]. Moreover, as demonstration of the absolute dependence on the proteasomes of the hydrolysis reaction, disappearance of substrate was completely prevented when PA28γ-20S particles were inhibited by epoxomicin or when the substrates were incubated alone (Supplementary Figure 7).

PA28γ modifies the patterns of peptides produced by 20S proteasome during hydrolysis of full-length proteins

In order to understand the modifications in the 20S proteasome proteolytic properties induced by the binding of PA28γ, the peptides generated from IGF-1 and MBP were analyzed by tandem mass spectrometry (MS/MS). By this approach, 171 and 279 individual peptides were identified from IGF-1 and MBP, respectively, ranging in length from 8 to 25 residues (shorter products were eliminated to reduce false-positive identification) and are listed in the Supplementary Table 2. Importantly, this analysis allowed accurate identification of products with the correct size to potentially bind (directly or after trimming by aminopeptidases) to MHC class I heterodimers, and therefore is of particular interest to evaluate the possible role of PA28γ in the context of cell-mediated immune responses.

Through this experimental approach, we also demonstrated that some peptides are exclusively released by one of the two proteasomal forms (i.e. 20S or PA28γ-20S particle). Remarkably, and somewhat unexpectedly (see Discussion), in the range of lengths taken into consideration, almost all the peptides generated in a specific way by only one form of proteasome were released by the 20S particle, while very few were produced exclusively in the presence of PA28γ (Supplementary Table 2). Thereafter, our analysis focused on more detailed characterization of the peptides generated in common by both 20S and PA28γ-20S particles. To this end, the relative amount of each product was assessed by comparing the corresponding ion intensities measured in sequential MS/MS analyses, according to a method we have validated previously [18, 51]. Briefly, ion intensities were used to quantify the relative amounts of single fragments generated from IGF-1 and MBP by 20S proteasome alone or when associated with PA28γ. The results of this analysis are shown in Figure 5 and show that several peptide products are released in vastly different amounts by the 20S and PA28γ-20S particles. In this case, the association with PA28γ was also found to cause a consistent reduction in the number of individual peptides released in greater quantities during degradation of IGF-1 and MBP by the 20S proteasome. Furthermore, to investigate the modifications in the cleavage specificities caused by the association of PA28γ with the

20S particle, we analyzed the relative frequency of the amino acids present on the two sides (positions from P4 to P4') of the peptide bonds, whose hydrolysis generated the peptides quantified by MS/MS. To analyze this, we compared the amino acid sequences involved in the generation (both at the N and at the C-ter) of peptides produced in greater amounts by 20S alone or by PA28γ-20S (Figure 5). Although limited to peptides longer than 7 residues, this analysis did not highlight any enrichment of basic amino acids in the P1 position in the presence of PA28γ (Supplementary Figure 8), in good agreement with the data obtained with fluorogenic peptides, which show that PA28γ does not stimulate only tryptic 20S activity.

PA28γ regulates intracellular level of MBP

To verify if what was observed *in vitro* was also reflected *in cellulo,* we took advantage of a particular isoform of MBP that has been shown to contain a nontraditional PY-Nuclear Localization Signal (NLS) in its sequence that allows its transport and accumulation at the nucleus [66]. The expression of the protein (carrying a Myc-tag to facilitate its detection by western blot) was ectopically induced from a plasmid in eukaryotic cells characterized by different levels of PA28γ expression. Specifically, we utilized the A375 human melanoma cell line, which expresses high basal amounts of PA28γ, and its derivative Cas9-A375 PA28γ-knockout line (A375 Crispr), obtained by the CRISPR/Cas9 system and characterized in detail previously [51]. As expected, the A375 Crispr clone shows no detectable amounts of PA28γ, regardless of whether MBP is present (Figure 6A). Crucially, when expressed in parallel in the two different clones (i.e. A375 WT and A375 Crispr), MBP accumulates over time to much higher levels in cells that do not express PA28γ compared to those expressing it. This effect is evident within 24 hours after transfection, but becomes very strong after 48 hours (Figure 6B and Supplementary Figure 9). As independent demonstration that PA28γ-dependent proteasomal activity is impaired in A375 Crispr cells, the intracellular amounts of p21, a well characterized PA28γ-20S proteasome substrate, were similarly increased in these cells (Figure 6C). To the best of our knowledge, this is the first time that the cellular levels of MBP have been shown to be dependent on the activity of PA28γ. Although the biological relevance of this observation needs still to be investigated in greater detail, this *in cellulo* data confirm the findings of our *in vitro* experiments.

Discussion

To shed light on the molecular mechanism of PA28γ activity, we initially assessed the effect of PA28γ on the hydrolysis of a panel of different fluorogenic short peptides (2-4 amino acids long) thus probing all three 20S proteasome active sites. Although initial reports indicated that PA28γ exerts its stimulatory effect only towards 20S trypsin-like activity [27, 28], subsequent studies also described strong activation of the other two proteasomal peptidase activities both *in vitro* [29, 30] and *in vivo [31]*. In accordance with these latter findings, our study showed that hydrolysis rates of 10 fluorogenic substrates were highly enhanced when PA28γ associated with the 20S particle. Importantly, this stimulatory effect was not restricted to tryptic activity, but clearly affected chymotryptic and caspasic proteasomal cleavage specificities. Moreover, the extent of 20S activation varied between 4- and 18-fold, with no clear preference for a proteasome catalytic site or a specific substrate size.

The most surprising finding of our study, however, arises from experiments characterizing the effects of PA28γ on the hydrolysis of several naturally or chemically unstructured proteins. It is known that, by virtue of the absence of tightly folded higher order structures, denatured proteins freely diffuse inside the proteolytic cavity of latent 20S particles, whose axial pores, through which substrates access the internal catalytic lumen and products exit from the particle, are obstructed by the N-terminal tails of the α subunits [67]. However, the latency of the 20S core particle not associated with activators (i.e. 19S, PA28, PA200) is not complete, because, even without artificial conditions that result in its activation [3], the 20S proteasome can degrade full-length proteins [18, 60], likely because of transitory and/or only limited gate opening [61]. Accordingly, when unfolded substrate proteins were incubated with 20S proteasomes the rates of appearance of new amino groups, generated as a consequence of hydrolysis of the peptide bonds in the substrate, were linear for up to 8 hours. The same linearity was also evident when substrates were degraded by PA28γ-20S particles, but in this case an impressive higher generation of new amino groups (varying between 3- and 10-fold, depending on the substrate) systematically took place at each time point. Crucially, this enhanced release of primary amino groups by PA28γ-20S proteasomes might result from either accelerated substrate hydrolysis caused by the activator or by a significant reduction in the size distribution of the peptide products generated, as in the case of the homolog PA28αβ [18]. Analysis of the size distributions of proteasomal products released during degradation of β-casein in the presence and absence of PA28γ, however, clearly disproves the second hypothesis. In fact, the chromatographic profiles of 20S and PA28γ-20S proteasome products appear nearly superimposable and, accordingly, the means and medians of product lengths are almost the same (4 and ~3 residues).

Since binding of PA28γ does not significantly modify the size distribution of peptide products released from casein by 20S proteasomes, it is therefore clear that the higher generation rates of NH_2 groups seen in Figure 1A must be truly indicative of an accelerated casein breakdown induced by the activator. Direct evidence that PA28γ strongly stimulates the rates of unfolded protein hydrolysis by 20S proteasome was obtained by monitoring the disappearance of undigested substrates in time-course *in vitro* degradation kinetics reactions. Such experiments unambiguously showed that binding of PA28γ transforms relatively latent proteases such as free 20S into an extremely active proteolytic enzyme that hydrolyzes unfolded proteins at greatly accelerated rates. Importantly, the stimulatory activity of PA28γ appears restricted only towards unfolded substrates, as shown by its inability to sustain degradation of native IGF-1 and α-lactalbumin. This last observation is not totally unexpected, since, unlike the 19S activator, PA28γ lacks the ATPase activity necessary to denature tightly folded higher order structures in protein substrates to allow access to the internal proteolytic cavity of the 20S degradative particle. In line with these *in vitro* findings, a nucleus-targeted isoform of MBP has been shown to accumulate over time at much higher levels in a melanoma cell line knocked out for PA28γ compared to the parental one that markedly expresses the activator. Although the biological relevance of this observation needs further investigation, this data is in agreement with the results of our *in vitro* experiments, and strongly suggests that PA28γ promotes proteasomal degradation of MBP *in vivo*.

Of note, several studies have demonstrated that PA28γ is able to increase *in vitro* and *in vivo* hydrolysis by 20S particles of some specific proteins such as SRC-3, p21, p16, p19, PTTG1, and HCV core protein [33-37]. Although all these proteins share the same characteristic of being completely or in large part intrinsically unstructured [64, 68, 69], it is generally believed that some very specific, yet to be identified, features in their amino acid sequence or in their residual folded structure may be responsible for their recognition and interaction with PA28γ [32]. Therefore, the enhanced degradation of these proteins induced by PA28γ is generally seen as an exception rather than as the normal consequence of an intrinsic feature of this proteasomal activator. On the contrary, the finding that proteasomal degradation of several totally unrelated proteins, which differ in terms of molecular weight, amino acid composition, and chemical properties (e.g. isoelectric point and hydrophobicity), but share the same absence of folded structures, is potently improved by PA28γ. This strongly suggests that stimulation of hydrolysis of unstructured proteins might represent a more general property of this activator. This molecular model appears even more reinforced by the observation that PA28γ does not enable 20S degradation of the folded counterparts of the denatured proteins. In view of the fact that several analyses indicate that a substantial fraction of eukaryotic proteome is composed of proteins which are completely or in large part intrinsically unstructured [70], and whose degradation seems to involve ubiquitin-independent mechanisms [71], it is therefore reasonable to speculate that PA28γ might play a much more significant and broad role in the pathway of protein

breakdown than previously believed. Further *in vivo* studies, possibly with selective inhibitors of PA28γ that are currently underway (O. Coux and S. Apcher, unpublished data) will be required to clarify this important point.

The present data are even more surprising in the light of results we obtained previously in a similar investigation characterizing the biochemical functions of PA28αβ [18]. In that study, PA28αβ was found to strongly reduce the mean and median sizes of proteasome products and to profoundly modify the sequences of peptides released without, however, increasing the overall rates of protein substrate breakdown. Therefore, the biochemical effects on protein degradation by 20S particles of PA28γ and PA28αβ seems to be rather opposed. Since PA28γ and PA28α and β share a high degree of homology, the molecular reasons underlying these differences in biochemical properties are likely to rely on the few divergent regions, namely the so-called homologue-specific inserts that connect helix 1 with helix 2 and which are not resolved in the X-ray structure of PA28α, presumably because they are flexible [6]. Furthermore, recent phylogenetic analyses indicate that PA28γ is most similar to the common ancestor of the PA28 activator family, and most likely retains its original functions, while PA28α and PA28β appeared later and evolved very rapidly to perform new tasks related to the γ-interferon inducible MHC class I system [72], although their role in adaptive responses to stressful conditions (e.g. oxidative stress) also seems very likely [19-24]. Moreover, biochemical characterization of a PA28γ homolog in *Dictyostelium discoideum* led to the conclusion that PA28γ-20S proteasomes could represent early unique nuclear proteases of eukaryotic cells [73]. On the basis of these considerations, one would be tempted to speculate that PA28γ could have maintained the ancient property of promoting degradation of unstructured long polypeptides and proteins, while the phylogenetically more recent PA28α and β lost the ability to stimulate protein hydrolysis to gain a more pronounced capacity to modify the spectrum of peptides released by proteasomes in a functional way to favor MHC class I antigen presentation. This hypothesis is corroborated by the results of mass spectrometry analysis of products in our study. In fact, the association of PA28γ with the 20S proteasome determines an evident reduction in the variability of peptide products that are potentially available for class I presentation, while PA28αβ activity is always correlated with enhancing the diversity of proteasomal products, in a way that makes it more likely that an appropriate CTL response is elicited [18, 74, 75].

References

1. Voges D, Zwickl P, Baumeister W. The 26S proteasome: A molecular machine designed for controlled proteolysis. Annual Review of Biochemistry. 1999;68:1015-68. doi: 10.1146/annurev.biochem.68.1.1015.
2. Baumeister W, Walz J, Zuhl F, Seemuller E. The proteasome: Paradigm of a self-compartmentalizing protease. Cell. 1998;92(3):367-80. doi: 10.1016/s0092-8674(00)80929-0.
3. Coux O, Tanaka K, Goldberg AL. Structure and functions of the 20S and 26S proteasomes. Annual Review of Biochemistry. 1996;65:801-47. doi: 10.1146/annurev.bi.65.070196.004101.
4. Goldberg AL, Cascio P, Saric T, Rock KL. The importance of the proteasome and subsequent proteolytic steps in the generation of antigenic peptides. Molecular Immunology. 2002;39(3-4):147-64. doi: 10.1016/s0161-5890(02)00098-6.
5. Harris JL, Alper PB, Li J, Rechsteiner M, Backes BJ. Substrate specificity of the human proteasome. Chemistry & Biology. 2001;8(12):1131-41. doi: 10.1016/s1074-5521(01)00080-1.
6. Rechsteiner M, Realini C, Ustrell V. The proteasome activator 11 S REG (PA28) and Class I antigen presentation. Biochemical Journal. 2000;345:1-15. doi: 10.1042/0264-6021:3450001.
7. Whitby FG, Masters EI, Kramer L, Knowlton JR, Yao Y, Wang CC, et al. Structural basis for the activation of 20S proteasomes by 11S regulators. Nature. 2000;408(6808):115-20. doi: 10.1038/35040607.
8. Stadtmueller BM, Hill CP. Proteasome Activators. Molecular Cell. 2011;41(1):8-19. doi: 10.1016/j.molcel.2010.12.020.
9. Xie SC, Metcalfe RD, Hanssen E, Yang T, Gillett DL, Leis AP, et al. The structure of the PA28-20S proteasome complex from Plasmodium falciparum and implications for proteostasis. Nature Microbiology. 2019;4(11):1990-2000. doi: 10.1038/s41564-019-0524-4.
10. Chen JH, Wang YF, Xu C, Chen KJ, Zhao QY, Wang ST, et al. Cryo-EM of mammalian PA28 alpha beta-iCP immunoproteasome reveals a distinct mechanism of proteasome activation by PA28 alpha beta. Nature Communications. 2021;12(1). doi: 10.1038/s41467-021-21028-3.
11. Lesne J, Locard-Paulet M, Parra J, Zivkovic D, Menneteau T, Bousquet MP, et al. Conformational maps of human 20S proteasomes reveal PA28-and immuno-dependent inter-ring crosstalks. Nature Communications. 2020;11(1). doi: 10.1038/s41467-020-19934-z.
12. Yu ZL, Yu YD, Wang F, Myasnikov AG, Coffino P, Cheng YF. Allosteric coupling between alpha-rings of the 20S proteasome. Nature Communications. 2020;11(1). doi: 10.1038/s41467-020-18415-7.

13. Huber EM, Groll M. The Mammalian Proteasome Activator PA28 Forms an Asymmetric alpha(4)beta(3) Complex. Structure. 2017;25(10):1473-+. doi: 10.1016/j.str.2017.07.013.

14. Cascio P. PA28αβ: the enigmatic magic ring of the proteasome? Biomolecules. 2014;4(2):566-84. doi: 10.3390/biom4020566.

15. Dubiel W, Pratt G, Ferrell K, Rechsteiner M. PURIFICATION OF AN 11-S REGULATOR OF THE MULTICATALYTIC PROTEASE. Journal of Biological Chemistry. 1992;267(31):22369-77.

16. Ma CP, Slaughter CA, Demartino GN. IDENTIFICATION, PURIFICATION, AND CHARACTERIZATION OF A PROTEIN ACTIVATOR (PA28) OF THE 20-S PROTEASOME (MACROPAIN). Journal of Biological Chemistry. 1992;267(15):10515-23.

17. Kuehn L, Dahlmann B. Proteasome activator PA28 and its interaction with 20 S proteasomes. Archives of Biochemistry and Biophysics. 1996;329(1):87-96. doi: 10.1006/abbi.1996.0195.

18. Raule M, Cerruti F, Benaroudj N, Migotti R, Kikuchi J, Bachi A, et al. PA28 alpha beta Reduces Size and Increases Hydrophilicity of 20S Immunoproteasome Peptide Products. Chemistry & Biology. 2014;21(4):470-80. doi: 10.1016/j.chembiol.2014.02.006.

19. Li J, Powell SR, Wang XJ. Enhancement of proteasome function by PA28 alpha overexpression protects against oxidative stress. Faseb Journal. 2011;25(3):883-93. doi: 10.1096/fj.10-160895.

20. Pickering AM, Linder RA, Zhang HQ, Forman HJ, Davies KJA. Nrf2-dependent Induction of Proteasome and Pa28 alpha beta Regulator Are Required for Adaptation to Oxidative Stress. Journal of Biological Chemistry. 2012;287(13):10021-31. doi: 10.1074/jbc.M111.277145.

21. Pickering AM, Davies KJA. Differential roles of proteasome and immunoproteasome regulators Pa28 alpha beta, Pa28 gamma and Pa200 in the degradation of oxidized proteins. Archives of Biochemistry and Biophysics. 2012;523(2):181-90. doi: 10.1016/j.abb.2012.04.018.

22. Hernebring M, Fredriksson A, Liljevald M, Cvijovic M, Norrman K, Wiseman J, et al. Removal of damaged proteins during ES cell fate specification requires the proteasome activator PA28. Scientific Reports. 2013;3. doi: 10.1038/srep01381.

23. Raynes R, Pomatto L, Davies K. Degradation of oxidized proteins by the proteasome: Distinguishing between the 20S, 26S, and immunoproteasome proteolytic pathways. Molecular Aspects of Medicine. 2016;50:41-55. doi: 10.1016/j.mam.2016.05.001.

24. Lobanova ES, Finkelstein S, Li J, Travis AM, Hao Y, Klingeborn M, et al. Increased proteasomal activity supports photoreceptor survival in inherited retinal degeneration. Nature Communications. 2018;9. doi: 10.1038/s41467-018-04117-8.

25. Sijts A, Sun YC, Janek K, Kral S, Paschen A, Schadendorf D, et al. The role of the proteasome activator PA28 in MHC class I antigen processing. Molecular Immunology. 2002;39(3-4):165-9. doi: 10.1016/s0161-5890(02)00099-8.

26. Cascio P. PA28 gamma: New Insights on an Ancient Proteasome Activator. Biomolecules. 2021;11(2). doi: 10.3390/biom11020228.

27. Realini C, Jensen CC, Zhang ZG, Johnston SC, Knowlton JR, Hill CP, et al. Characterization of recombinant REG alpha, REG beta, and REG gamma proteasome activators. Journal of Biological Chemistry. 1997;272(41):25483-92. doi: 10.1074/jbc.272.41.25483.

28. Zhang ZG, Clawson A, Rechsteiner M. The proteasome activator 11 S regulator or PA28 - Contribution by both alpha and beta subunits to proteasome activation. Journal of Biological Chemistry. 1998;273(46):30660-8. doi: 10.1074/jbc.273.46.30660.

29. Wilk S, Chen WE, Magnusson RP. Properties of the beta subunit of the proteasome activator PA28 (11S REG). Archives of Biochemistry and Biophysics. 2000;384(1):174-80. doi: 10.1006/abbi.2000.2112.

30. Jonik-Nowak B, Menneteau T, Fesquet D, Baldin V, Bonne-Andrea C, Mechali F, et al. PIP30/FAM192A is a novel regulator of the nuclear proteasome activator PA28 gamma. Proceedings of the National Academy of Sciences of the United States of America. 2018;115(28):E6477-E86. doi: 10.1073/pnas.1722299115.

31. Huang L, Haratake K, Miyahara H, Chiba T. Proteasome activators, PA28 gamma and PA200, play indispensable roles in male fertility. Scientific Reports. 2016;6. doi: 10.1038/srep23171.

32. Mao I, Liu J, Li X, Luo H. REGgamma, a proteasome activator and beyond? Cell Mol Life Sci. 2008;65(24):3971-80. doi: 10.1007/s00018-008-8291-z.

33. Li XT, Lonard DM, Jung SY, Malovannaya A, Feng G, Qin J, et al. The SRC-3/AIB1 coactivator is degraded 14 in a ubiquitin- and ATP-independent manner by the REG gamma proteasome. Cell. 2006;124(2):381-92. doi: 10.1016/j.cell.2005.11.037.

34. Moriishi K, Okabayashi T, Nakai K, Moriya K, Koike K, Murata S, et al. Proteasome activator PA28 gamma-dependent nuclear retention and degradation of hepatitis C virus core protein. Journal of Virology. 2003;77(19):10237-49. doi: 10.1128/jvi.77.19.10237-10249.2003.

35. Ying H, Furuya F, Zhao L, Araki O, West BL, Hanover JA, et al. Aberrant accumulation of PTTG1 induced by a mutated thyroid hormone beta receptor inhibits mitotic progression. Journal of Clinical Investigation. 2006;116(11):2972-84. doi: 10.1172/jci28598.

36. Li XT, Amazit L, Long W, Lonard DM, Monaco JJ, O'Malley BW. Ubiquitin- and ATP-independent proteolytic turnover of p21 by the REG gamma-proteasome pathway. Molecular Cell. 2007;26(6):831-42. doi: 10.1016/j.molcel.2007.05.028.

37. Chen XY, Barton LF, Chi Y, Clurman BE, Roberts JM. Ubiquitin-independent degradation of cell-cycle inhibitors by the REG gamma proteasome. Molecular Cell. 2007;26(6):843-52. doi: 10.1016/j.molcel.2007.05.022.

38. Zhang Z, Zhang RW. Proteasome activator PA28 gamma regulates p53 by enhancing its MDM2-mediated degradation. Embo Journal. 2008;27(6):852-64. doi: 10.1038/emboj.2008.25.

39. Murata S, Kawahara H, Tohma S, Yamamoto K, Kasahara M, Nabeshima Y, et al. Growth retardation in mice lacking the proteasome activator PA28 gamma. Journal of Biological Chemistry. 1999;274(53):38211-5. doi: 10.1074/jbc.274.53.38211.

40. Masson P, Lundgren J, Young P. Drosophila proteasome regulator REG gamma: Transcriptional activation by DNA replication-related factor DREF and evidence for a role in cell cycle progression. Journal of Molecular Biology. 2003;327(5):1001-12. doi: 10.1016/s0022-2836(03)00188-8.

41. Barton LF, Runnels HA, Schell TD, Cho YJ, Gibbons R, Tevethia SS, et al. Immune defects in 28-kDa proteasome activator gamma-deficient mice. Journal of Immunology. 2004;172(6):3948-54. doi: 10.4049/jimmunol.172.6.3948.

42. Zannini L, Lecis D, Buscemi G, Carlessi L, Gasparini P, Fontanella E, et al. REG gamma proteasome activator is involved in the maintenance of chromosomal stability. Cell Cycle. 2008;7(4):504-12. doi: 10.4161/cc.7.4.5355.

43. Cioce M, Boulon S, Matera AG, Lamond AI. UV-induced fragmentation of Cajal bodies. Journal of Cell Biology. 2006;175(3):401-13. doi: 10.1083/jcb.200604099.

44. Zannini L, Buscemi G, Fontanella E, Lisanti S, Delia D. REG gamma/PA28 gamma proteasome activator interacts with PML and Chk2 and affects PML nuclear bodies number. Cell Cycle. 2009;8(15):2399-407. doi: 10.4161/cc.8.15.9084.

45. Levy-Barda A, Lerenthal Y, Davis AJ, Chung YM, Essers J, Shao ZP, et al. Involvement of the nuclear proteasome activator PA28 gamma in the cellular response to DNA double-strand breaks. Cell Cycle. 2011;10(24):4300-10. doi: 10.4161/cc.10.24.18642.

46. Dong SX, Jia CF, Zhang SP, Fan GJ, Li YB, Shan PP, et al. The REG gamma Proteasome Regulates Hepatic Lipid Metabolism through Inhibition of Autophagy. Cell Metabolism. 2013;18(3):380-91. doi: 10.1016/j.cmet.2013.08.012.

47. Chen DB, Yang XS, Huang LY, Chi P. The Expression and Clinical Significance of PA28 gamma in Colorectal Cancer. Journal of Investigative Medicine. 2013;61(8):1192-6.

48. Li L, Dang YY, Zhang JS, Yan WJ, Zhai WL, Chen H, et al. REG gamma is critical for skin carcinogenesis by modulating the Wnt/beta-catenin pathway. Nature Communications. 2015;6. doi: 10.1038/ncomms7875.

49. He J, Cui L, Zeng Y, Wang GQ, Zhou P, Yang YY, et al. REG gamma is associated with multiple oncogenic pathways in human cancers. Bmc Cancer. 2012;12. doi: 10.1186/1471-2407-12-75.

50. Yao LF, Zhou L, Xuan Y, Zhang P, Wang XS, Wang TZ, et al. The proteasome activator REG gamma counteracts immunoproteasome expression and autoimmunity. Journal of Autoimmunity. 2019;103. doi: 10.1016/j.jaut.2019.05.010.

51. Boulpicante M, Darrigrand R, Pierson A, Salgues V, Rouillon M, Gaudineau B, et al. Tumors escape immunosurveillance by overexpressing the proteasome activator PSME3. Oncoimmunology. 2020;9(1). doi: 10.1080/2162402x.2020.1761205.

52. Le Feuvre A, Dantas-Barbosa C, Baldin V, Coux O. High yield bacterial expression and purification of active recombinant PA28 alpha beta complex. Protein Expression and Purification. 2009;64(2):219-24. doi: 10.1016/j.pep.2008.10.014.

53. Cerruti F, Martano M, Petterino C, Bollo E, Morello E, Bruno R, et al. Enhanced expression of interferon-gamma-induced antigen-processing machinery components in a spontaneously occurring cancer. Neoplasia. 2007;9(11):960-9. doi: 10.1593/neo.07649.

54. Raule M, Cerruti F, Cascio P. Enhanced rate of degradation of basic proteins by 26S immunoproteasomes. Biochimica Et Biophysica Acta-Molecular Cell Research. 2014;1843(9):1942-7. doi: 10.1016/j.bbamcr.2014.05.005.

55. Akopian TN, Kisselev AF, Goldberg AL. Processive degradation of proteins and other catalytic properties of the proteasome from Thermoplasma acidophilum. Journal of Biological Chemistry. 1997;272(3):1791-8. doi: 10.1074/jbc.272.3.1791.

56. Rappsilber J, Mann M, Ishihama Y. Protocol for micro-purification, enrichment, pre-fractionation and storage of peptides for proteomics using StageTips. Nature Protocols. 2007;2(8):1896-906. doi: 10.1038/nprot.2007.261.

57. Perez-Riverol Y, Csordas A, Bai J, Bernal-Llinares M, Hewapathirana S, Kundu D, et al. The PRIDE database and related tools and resources in 2019: improving support for quantification data. Nucleic Acids Research. 2019;47(D1):D442-D50. doi: 10.1093/nar/gky1106.

58. Dolenc I, Seemuller E, Baumeister W. Decelerated degradation of short peptides by the 20S proteasome. Febs Letters. 1998;434(3):357-61. doi: 10.1016/s0014-5793(98)01010-2.

59. Saric T, Graef CI, Goldberg AL. Pathway for degradation of peptides generated by proteasomes - A key role for thimet oligopeptidase and other metallopeptidases. Journal of Biological Chemistry. 2004;279(45):46723-32. doi: 10.1074/jbc.M406537200.

60. Kisselev AF, Akopian TN, Goldberg AL. Range of sizes of peptide products generated during degradation of different proteins by archaeal proteasomes. Journal of Biological Chemistry. 1998;273(4):1982-9. doi: 10.1074/jbc.273.4.1982.

61. Kohler A, Cascio P, Leggett DS, Woo KM, Goldberg AL, Finley D. The axial channel of the proteasome core particle is gated by the Rpt2 ATPase and controls both substrate entry and product release. Molecular Cell. 2001;7(6):1143-52. doi: 10.1016/s1097-2765(01)00274-x.

62. Emmerich NPN, Nussbaum AK, Stevanovic S, Priemer M, Toes REM, Rammensee HG, et al. The human 26 S and 20 S proteasomes generate overlapping but different sets of peptide fragments from a model protein substrate. Journal of Biological Chemistry. 2000;275(28):21140-8. doi: 10.1074/jbc.M000740200.

63. Kisselev AF, Akopian TN, Woo KM, Goldberg AL. The sizes of peptides generated from protein by mammalian 26 and 20 S proteasomes - Implications for understanding the degradative mechanism and antigen presentation. Journal of Biological Chemistry. 1999;274(6):3363-71. doi: 10.1074/jbc.274.6.3363.

64. Zhou PB. REG gamma: A shortcut to destruction. Cell. 2006;124(2):256-7. doi: 10.1016/j.cell.2006.01.003.

65. Cascio P, Hilton C, Kisselev AF, Rock KL, Goldberg AL. 26S proteasomes and immunoproteasomes produce mainly N-extended versions of an antigenic peptide. Embo Journal. 2001;20(10):2357-66. doi: 10.1093/emboj/20.10.2357.

66. Smith G, Seymour L, Boggs J, Harauz G. The 21.5-kDa isoform of myelin basic protein has a non-traditional PY-nuclear-localization signal. Biochemical and Biophysical Research Communications. 2012;422(4):670-5. doi: 10.1016/j.bbrc.2012.05.051.

67. Groll M, Bajorek M, Kohler A, Moroder L, Rubin DM, Huber R, et al. A gated channel into the proteasome core particle. Nature Structural Biology. 2000;7(11):1062-7. doi: 10.1038/80992.

68. Sanchez-Puig N, Veprintsev DB, Fersht AR. Human full-length Securin is a natively unfolded protein. Protein Science. 2005;14(6):1410-8. doi: 10.1110/ps.051368005.

69. Duvignaud JB, Savard C, Fromentin R, Majeau N, Leclerc D, Gagne SM. Structure and dynamics of the N-terminal half of hepatitis C virus core protein: An intrinsically unstructured protein. Biochemical and Biophysical Research Communications. 2009;378(1):27-31. doi: 10.1016/j.bbrc.2008.10.141.

70. Peng ZL, Mizianty MJ, Kurgan L. Genome-scale prediction of proteins with long intrinsically disordered regions. Proteins-Structure Function and Bioinformatics. 2014;82(1):145-58. doi: 10.1002/prot.24348.

71. Tsvetkov P, Reuven N, Shaul Y. The nanny model for IDPs. Nature Chemical Biology. 2009;5(11):778-81. doi: 10.1038/nchembio.233.

72. Fort P, Kajava AV, Delsuc F, Coux O. Evolution of Proteasome Regulators in Eukaryotes. Genome Biology and Evolution. 2015;7(5):1363-79. doi: 10.1093/gbe/evv068.

73. Masson P, Lundin D, Soderbom F, Young P. Characterization of a REG/PA28 Proteasome Activator Homolog in Dictyostelium discoideum Indicates that the Ubiquitin- and ATP-Independent REG gamma Proteasome Is an Ancient Nuclear Protease. Eukaryotic Cell. 2009;8(6):844-51. doi: 10.1128/ec.00165-08.

74. Cascio P, Call M, Petre BM, Walz T, Goldberg AL. Properties of the hybrid form of the 26S proteasome containing both 19S and PA28 complexes. Embo Journal. 2002;21(11):2636-45. doi: 10.1093/emboj/21.11.2636.

75. Groettrup M, Ruppert T, Kuehn L, Seeger M, Standera S, Koszinowski U, et al. The interferon-gamma-inducible 11 S regulator (PA28) and the LMP2/LMP7 subunits govern the peptide production by the 20 S proteasome in vitro. J Biol Chem. 1995;270(40):23808-15. doi: 10.1074/jbc.270.40.23808.

Figure Captions

Fig. 1 Increased rates of peptide bond cleavage and size distribution of peptides generated during hydrolysis of casein by PA28γ-20S proteasomes. **A** β-casein was incubated with 20S and PA28γ-20S proteasomes and the amino groups released, as a consequence of the degradation of the substrate, were measured with the fluorescamine at the indicated time points. Data are the average of three independent experiments (four for time 8 hr) ± SEM. Appearance of amino groups was totally abrogated in presence of 20 μM of the highly specific proteasome inhibitor epoxomicin. *** P <0.001. **B** Equal amounts of peptides generated during degradation of casein by 20S and PA28γ-20S proteasomes were reacted with fluorescamine and immediately fractionated by HP-SEC. Data are representative of four independent experiments. **C** Mean and median peptide sizes generated by 20S and PA28γ-20S proteasomes from casein were calculated using the product distributions obtained by HP-SEC, assuming an average molecular weight of 110 Da for each residue. Values are the average of four experiments (±SEM)

Fig. 2 Increased rates of peptide bond cleavage during hydrolysis of different unfolded proteins by PA28γ-20S proteasomes. MBP, IGF-1, and α-lactalbumin were incubated with 20S and PA28γ-20S proteasomes and the amino groups released were measured with the fluorescamine as in Figure 1. Data are the average of three to six independent experiments ± SEM. *** P <0.001

Fig. 3 PA28γ promotes proteasomal degradation of unfolded proteins but not of their native counterparts. Native and denatured IGF-1 (upper panel) and α-lactalbumin (lower panel) were incubated with PA28γ-20S proteasomes and the amino groups released, as a consequence of the degradation of the substrate, were measured with fluorescamine at the indicated time points. Data are the average of three to five independent experiments ± SEM. *** P <0.001

Fig. 4 Enhanced rates of MBP, IGF-1, and α-lactalbumin proteasomal hydrolysis induced by PA28γ but not by PA28αβ. MBP **A,** IGF-1 **B,** and α-lactalbumin **C** were incubated as indicated in the figure, and the undegraded protein was separated by SDS-PAGE. Note that in the MBP gel the bands corresponding to enzymes cannot be appreciated since they were used at lower concentrations (see Materials and Methods for further details). **D** Densitometric quantification of the residual protein. Data are the average of three to four independent experiments (±SD). *** P <0.001

Fig. 5 MS/MS differential analysis of peptides generated during hydrolysis of IGF-1 and MBP by 20S and PA28γ-20S particles. Heatmap comparison of the abundance of significant peptides generated after 6 hours of proteasomal

degradation of IGF-1 and MBP in the 20S (biological and technical replicates of samples designated A, B, and C) and PA28γ-20S (biological and technical replicates of samples designated 1, 2, and 3) samples. Samples were analyzed by nLC-MS/MS and processed by MaxQuant against the database IGF-1 or MBP + contaminant sequences. Differences and similarities in peptide intensities (normalized to the Z-score) are shown; green indicates decreased levels, and red indicates increased levels. Data were obtained from supervised hierarchical clustering analysis by applying a t-test, Benjamini Hochberg correction, and a p-value of 0.05

Figure 6 Knockout of PA28γ results in accumulation of a nucleus-targeted MBP isoform in cell. **A** The expression of PA28γ was assessed by western blotting in A375 and A375 Crispr melanoma cells. The intensity of each band was normalized to that of the corresponding β-actin band, and the value related to that of the control (A375 expressing MBP) set as one. Experiments were performed in triplicate and data are expressed as mean ± SE. **B** Expression levels of MBP was assessed by WB with an anti-Myc-tag antibody, and data are presented as in (**A**). **C** Expression of p21 was verified by WB and indicated as in (**A**). * $P < 0.05$

Supplementary Fig. 1 Purified PA28γ and PA28αβ elute from Sephacryl S-200 gel filtration column as a complex of apparent molecular weight of about 200 kDa. ~150 µg of the final preparation of PA28γ **A** and PA28αβ **B** were analyzed by size exclusion chromatography on a calibrated Sephacryl S-200 column. The final preparation of PA28αβ consists of a heteroheptameric complex containing both the α and β subunits **C** and is able to strongly enhance the chymotryptic activity of 20S proteasome at picomolar concentrations **D**

Supplementary Fig. 2 Effects of increasing concentrations of PA28γ on the hydrolysis of different fluorogenic substrates by 20S peptidase activities. Proteasome chymotrypsin-like **A**, tryptic-like **B**, and caspase-like **C** activities were probed with the indicated fluorogenic peptides in the presence of increasing concentrations of PA28γ and expressed as fold activation compared to the activity of 20S alone. $R^2 \geq 0.9$ in all cases

Supplementary Fig. 3 PA28γ is unable to stimulate proteasomal degradation of two tryptic substrates. **A** Hydrolysis rates of 100 µM Z-LR-amc and Z-FR-amc were assessed in the presence of increasing concentration of PA28γ and displayed as in Figure 1. **B** Specific activities of 20S proteasomes were assessed at 100 and 250 µM concentrations of each substrate. * $P < 0.05$

Supplementary Fig. 4 Absolute dependence on proteasome proteolytic activity of β-casein hydrolysis. NH_2 generation was completely absent when the substrate was incubated alone **A** or with only PA28γ **B**

Supplementary Fig. 5 Calibration curve for the polyhydroxyethyl aspartamide size exclusion column using fluorescamine-derivatized amino acid and peptide molecular weight standards. The typical peak width of these amino acids and peptides was 0.7 min

Supplementary Fig. 6 Absolute dependence on proteasome proteolytic activity of MBP, IGF-1, and α-lactalbumin hydrolysis. NH_2 generation was completely absent when the substrates were incubated alone (**left panels**) or with only PA28γ (**right panels**)

Supplementary Fig. 7 Absolute dependence on the proteasome proteolytic activity of MBP, IGF-1, and α-lactalbumin hydrolysis. MBP **A**, IGF-1 **B**, and α-lactalbumin **C** were incubated alone or in the presence of PA28γ-20S proteasomes inhibited by 20 μM epoxomicin and analyzed as in Figure 4

Supplementary Fig. 8 Relative frequencies of amino acids surrounding the peptide bonds preferentially hydrolyzed by the 20S and PA28γ-20S proteasomes. Logos sequences were generated using WebLogo 3 (available at http://weblogo.threeplusone.com/), and refer to the cleavage sequences (Positions from P4 to P4 ') of the peptides generated in greater amounts by PA28γ-20S (left) and 20S proteasome (right) during the hydrolysis of IGF-1 and MBP. The colors of amino acids are based on their chemical properties: Polar (G, S, T, Y, C) green, Neutral (Q,N) purple, Basic (K,R,H) blue, Acidic (D,E) red, Hydrophobic (A,V,L,I,P,W,F,M) black

Supplementary Fig. 9 Knockout of PA28γ results in accumulation of MBP in cells. The expression of nucleus-targeted MBP was assessed with a specific antibody by western blotting in A375 and A375 Crispr melanoma cells, and β-actin was used as a loading control. At 24 hours post-transfection, accumulation of MBP can be noted which becomes increasingly evident after 48 hours

A

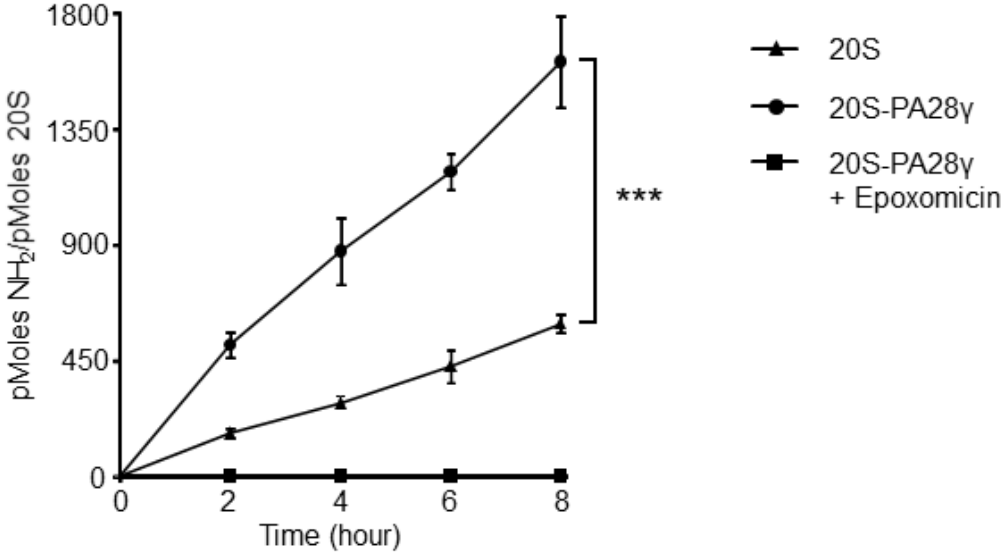

B

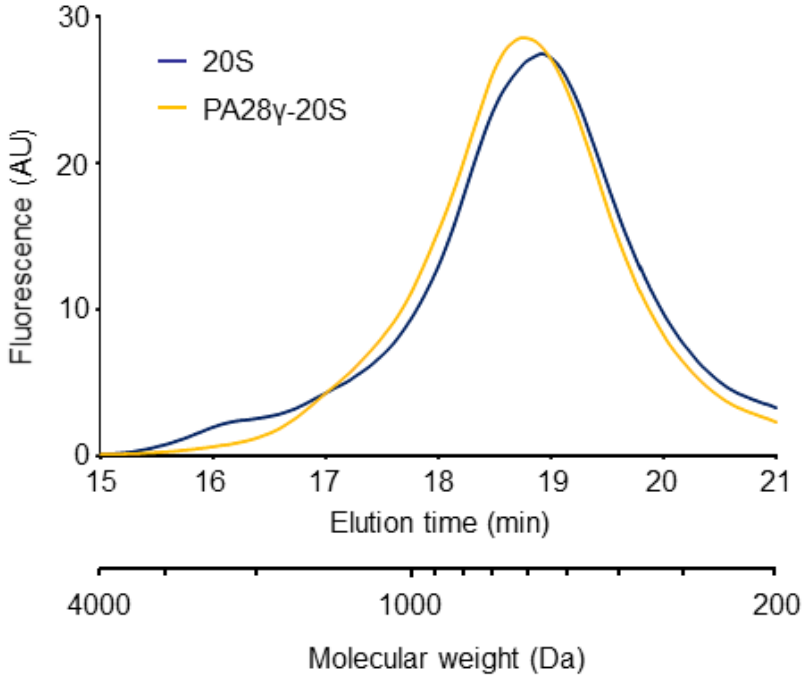

C

Proteasome	Mean	Median
20S	4.1 ± 0.07	3.1 ± 0.03
PA28γ-20S	4.0 ± 0.04	3.3 ± 0.03

Fig. 1

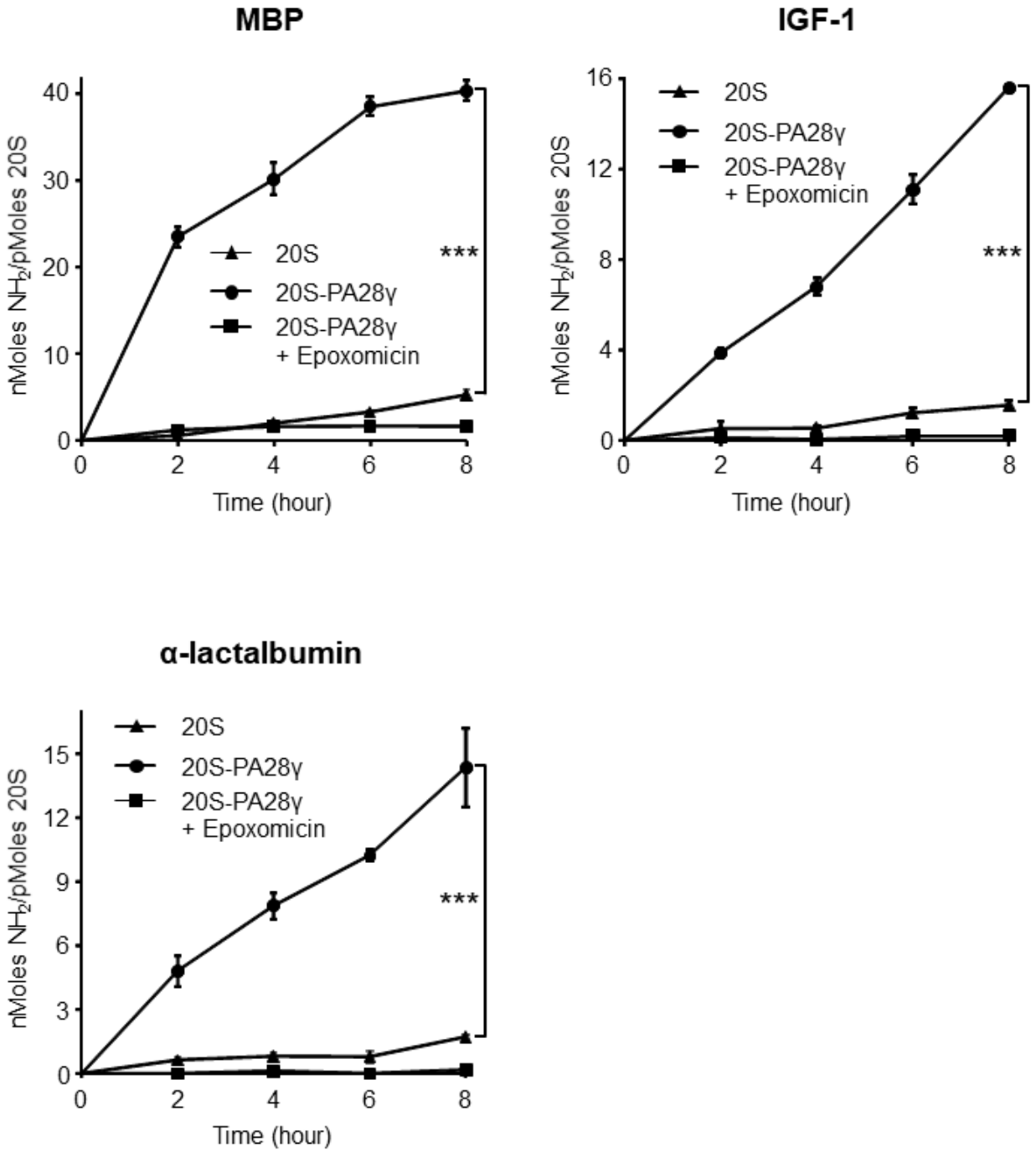

Fig. 2

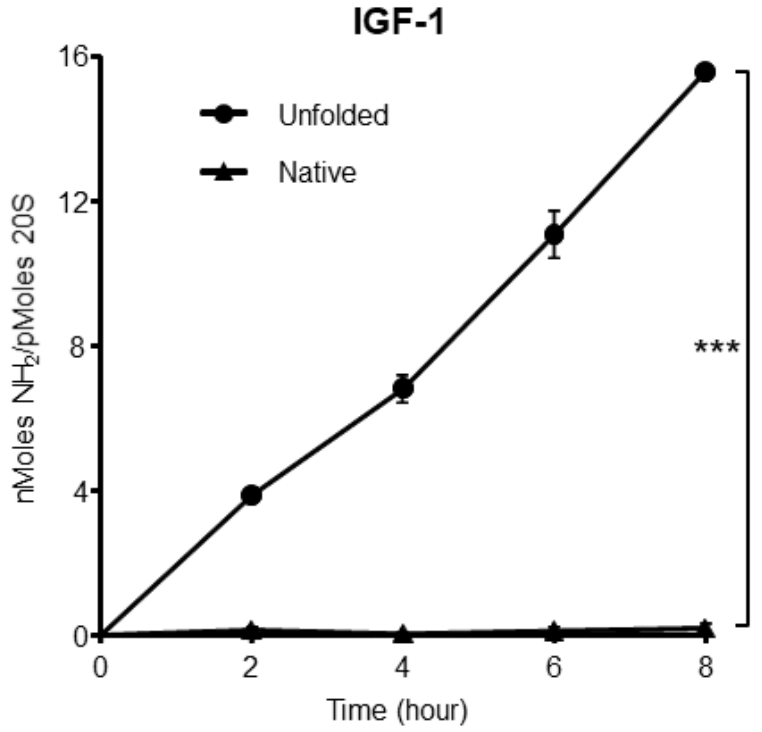

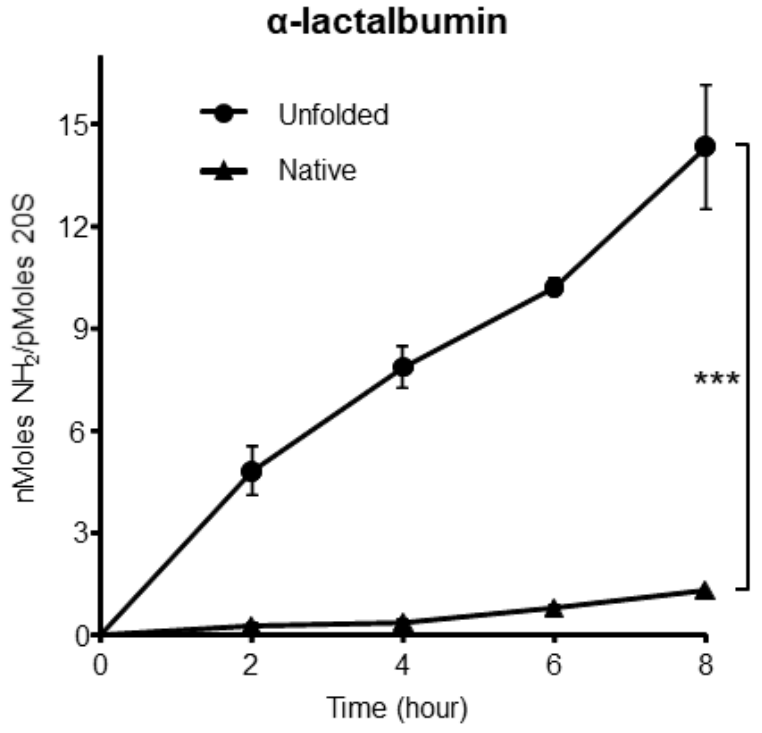

Fig. 3

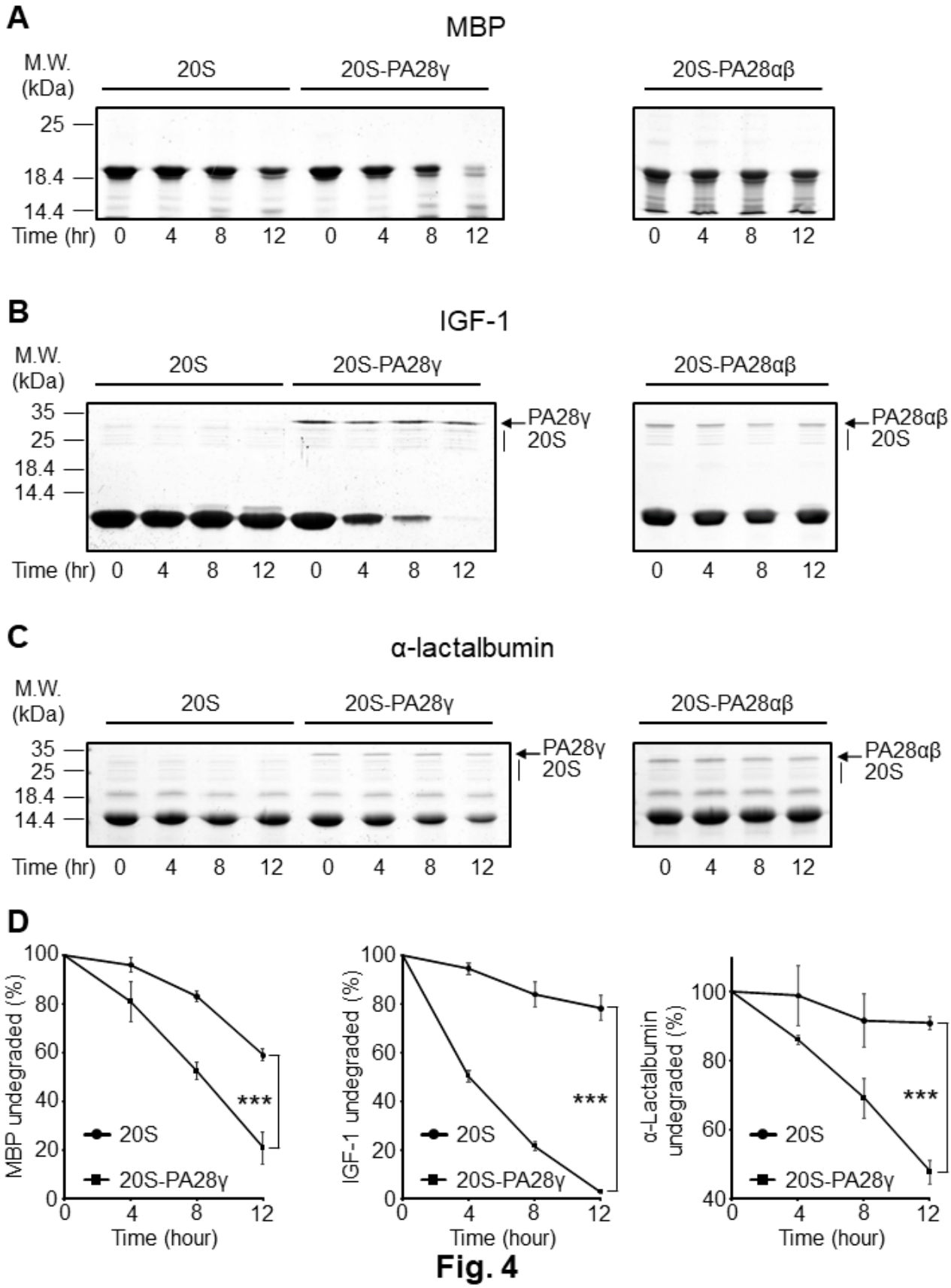

Fig. 4

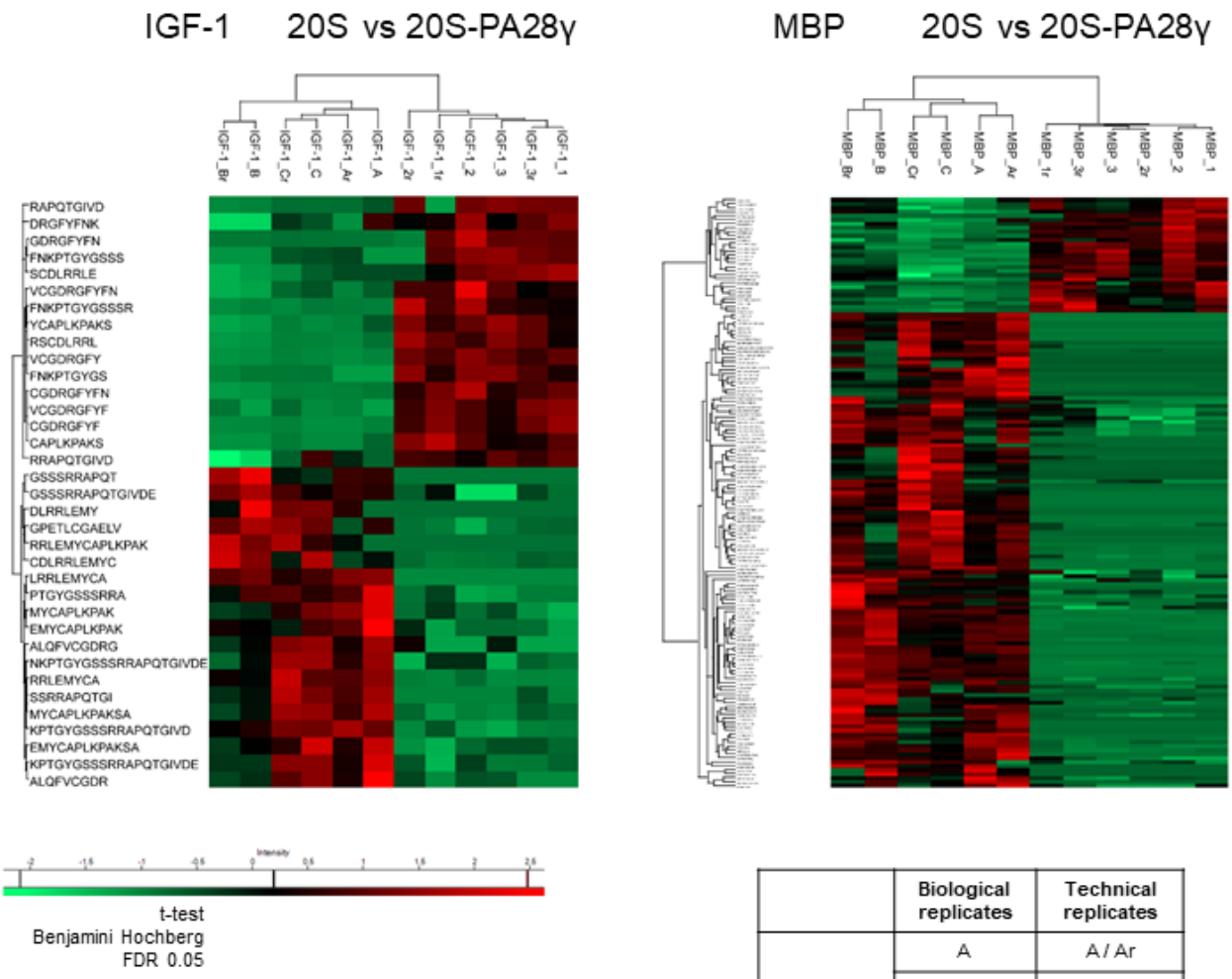

	Biological replicates	Technical replicates
20S	A	A / Ar
	B	B / Br
	C	C / Cr
20S-PA28γ	1	1 / 1r
	2	2 / 2r
	3	3 / 3r

Fig. 5

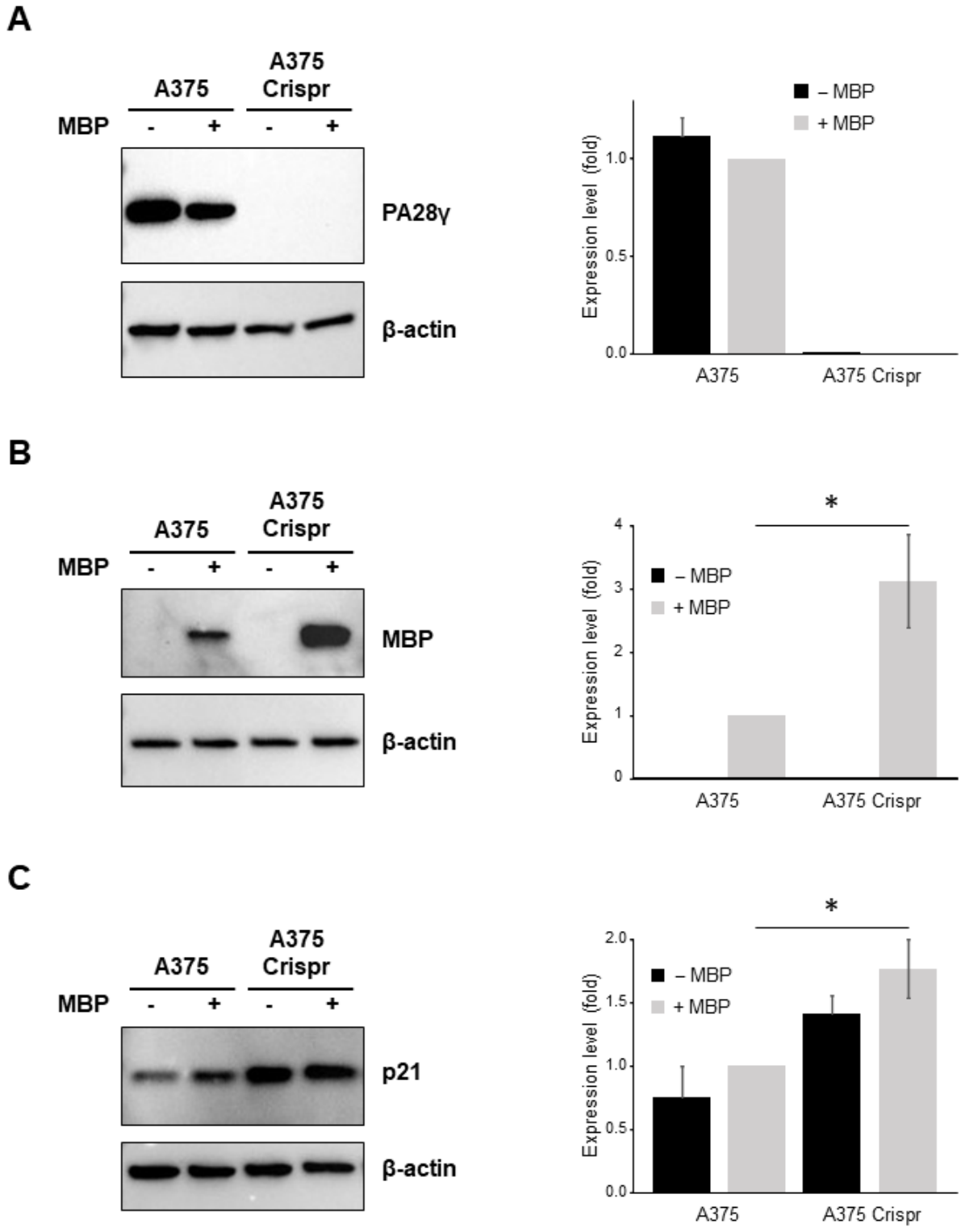

Fig. 6

		Maximum stimulation of 20S activities by PA28γ	
Proteasomal activity	Substrate	Fold	20S maximum specific activity (nmol peptide cleaved /mg * min)
Chymotrypsin-like	Suc-LLVY-amc	18,2	223,7
	Suc-LY-amc	4,3	62,6
	Suc-GGL-amc	3,8	368,6
	Suc-AAF-amc	6,7	264,1
Caspase-like	Suc-YVAD-amc	10,2	29,0
	Suc-DEVD-amc	6,7	7,0
Trypsin-like	Bz-VGR-amc	7,3	444,6
	Z-ARR-amc	4,3	134,8
	Boc-LRR-amc	16,5	411,0
	Z-RR-amc	6,1	1,9

Table 1 PA28γ kinetic parameters. Maximum PA28γ stimulation of 20S proteasome peptidase activities was calculated as described in the Materials and Methods from the curves shown in Supplementary Figure 2.

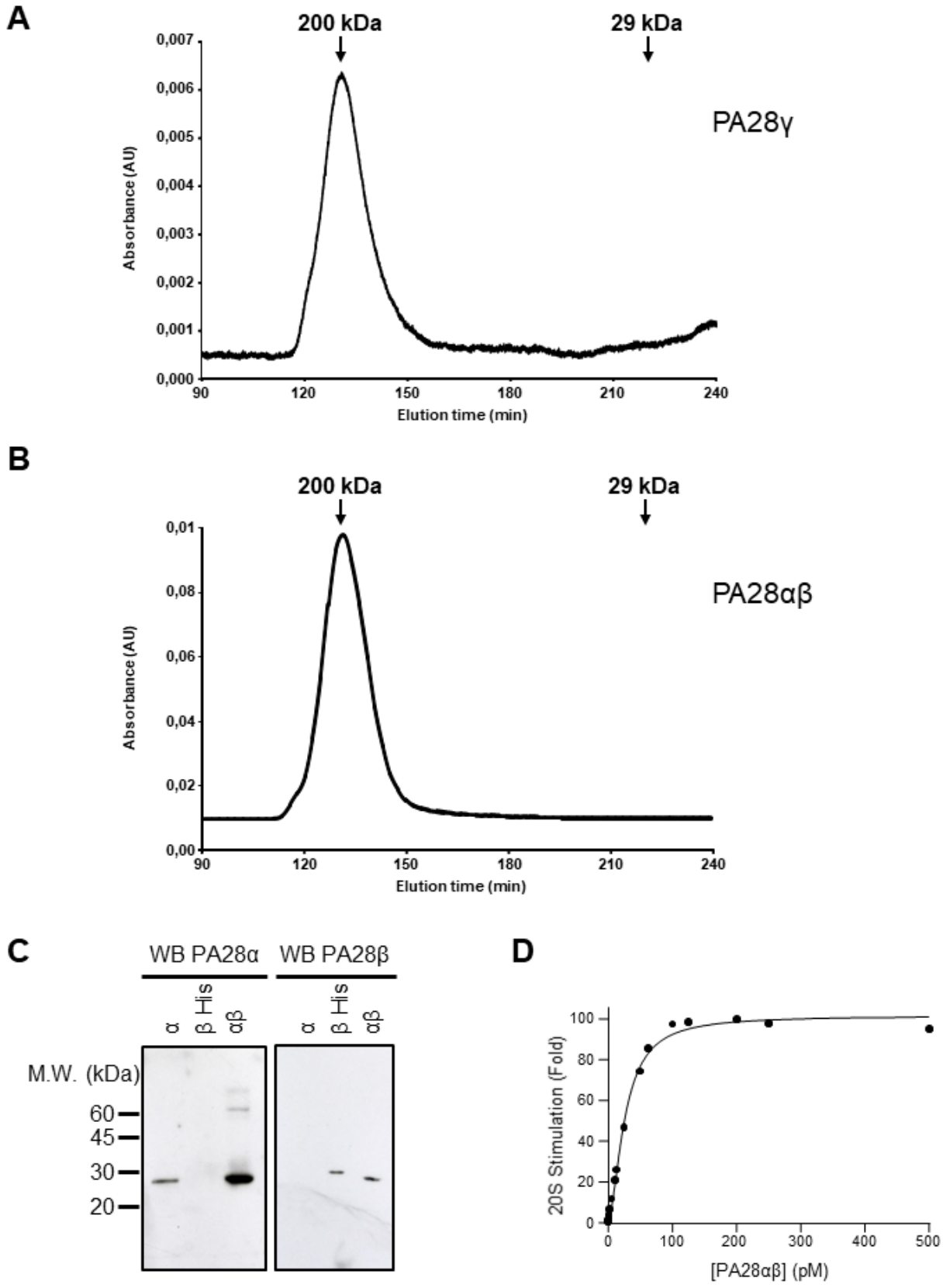

Supplementary Fig. 1

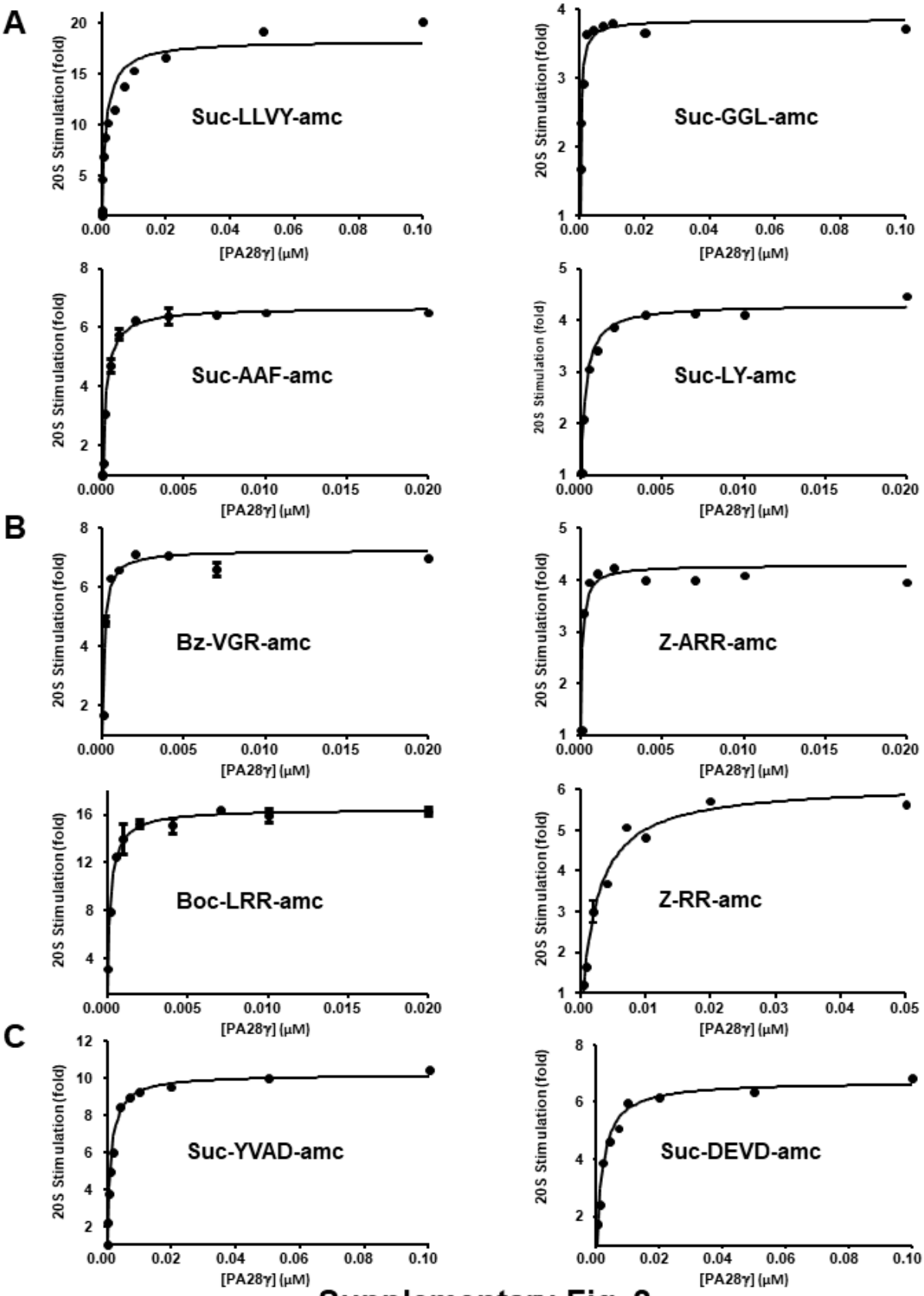

Supplementary Fig. 2

A

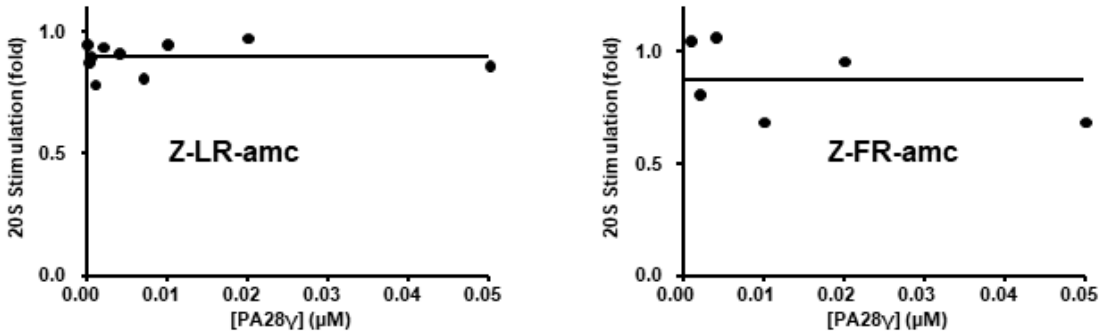

B

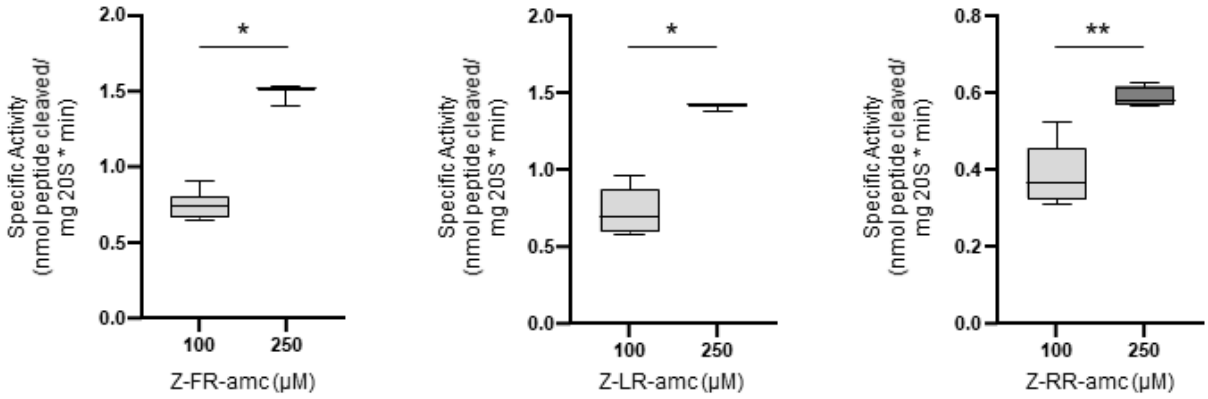

Supplementary Fig. 3

A

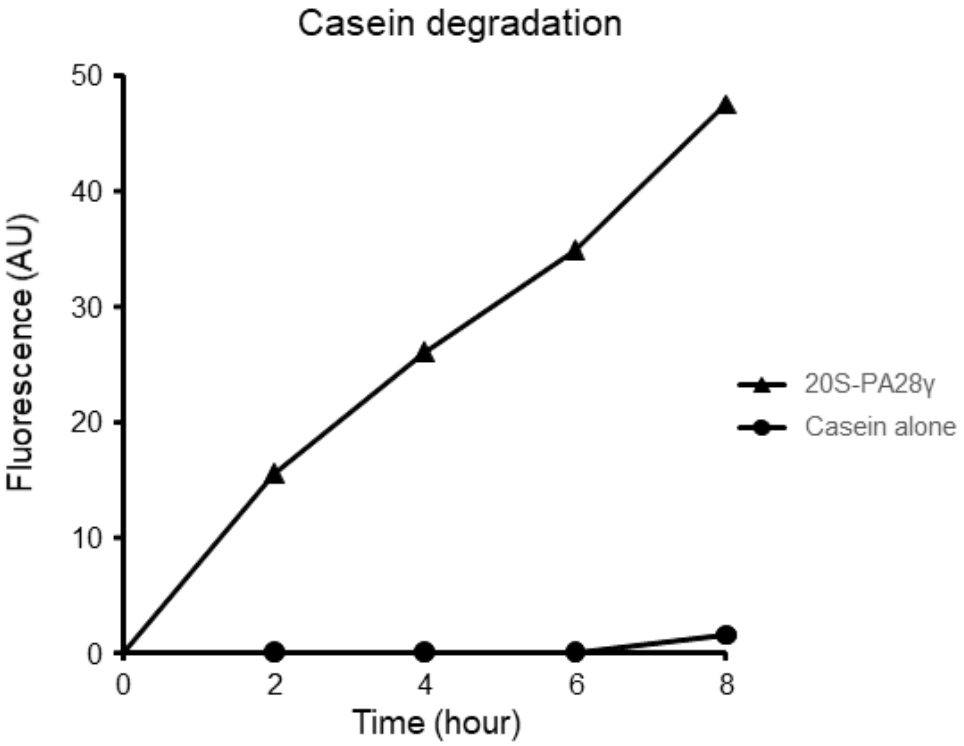

B

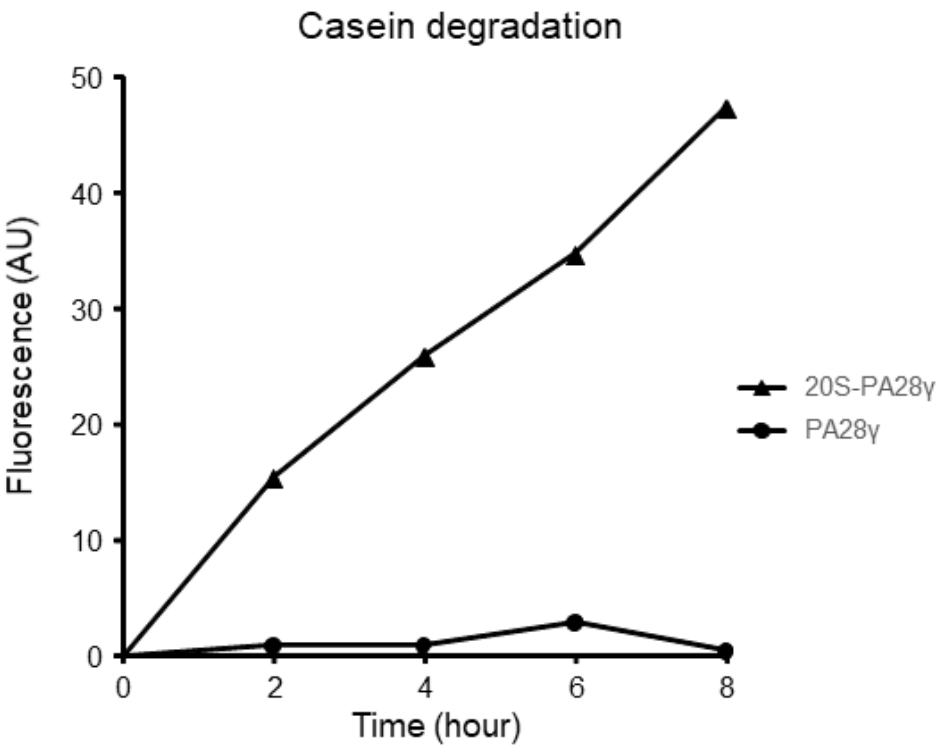

Supplementary Fig. 4

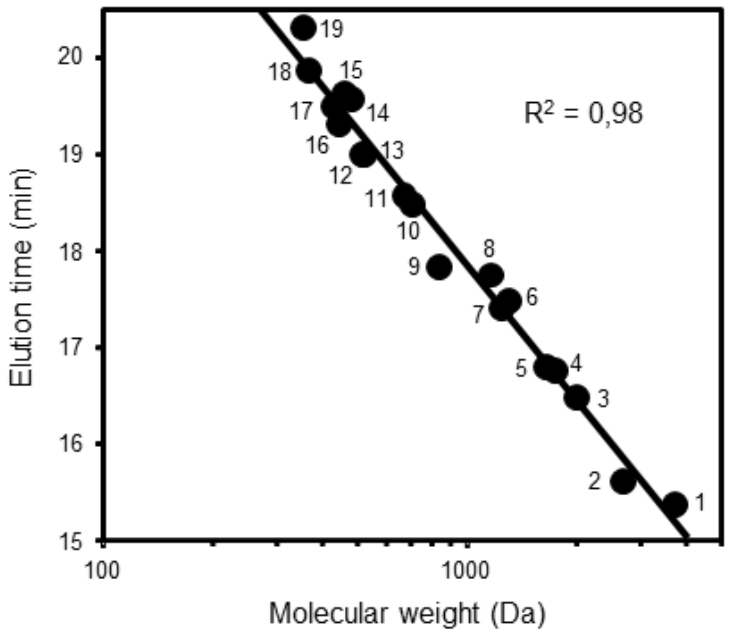

1	INSULIN B
2	INSULIN A
3	SGLEQLESIINFEKL
4	EQLESIINFEKL
5	VQIASNENMETM
6	ASNENMETM
7	SIINFEKL
8	IINFEKL
9	YGGFL
10	AGFM
11	GGFL
12	LGG
13	FA
14	W
15	Y
16	F
17	M
18	A
19	G

Supplementary Fig. 5

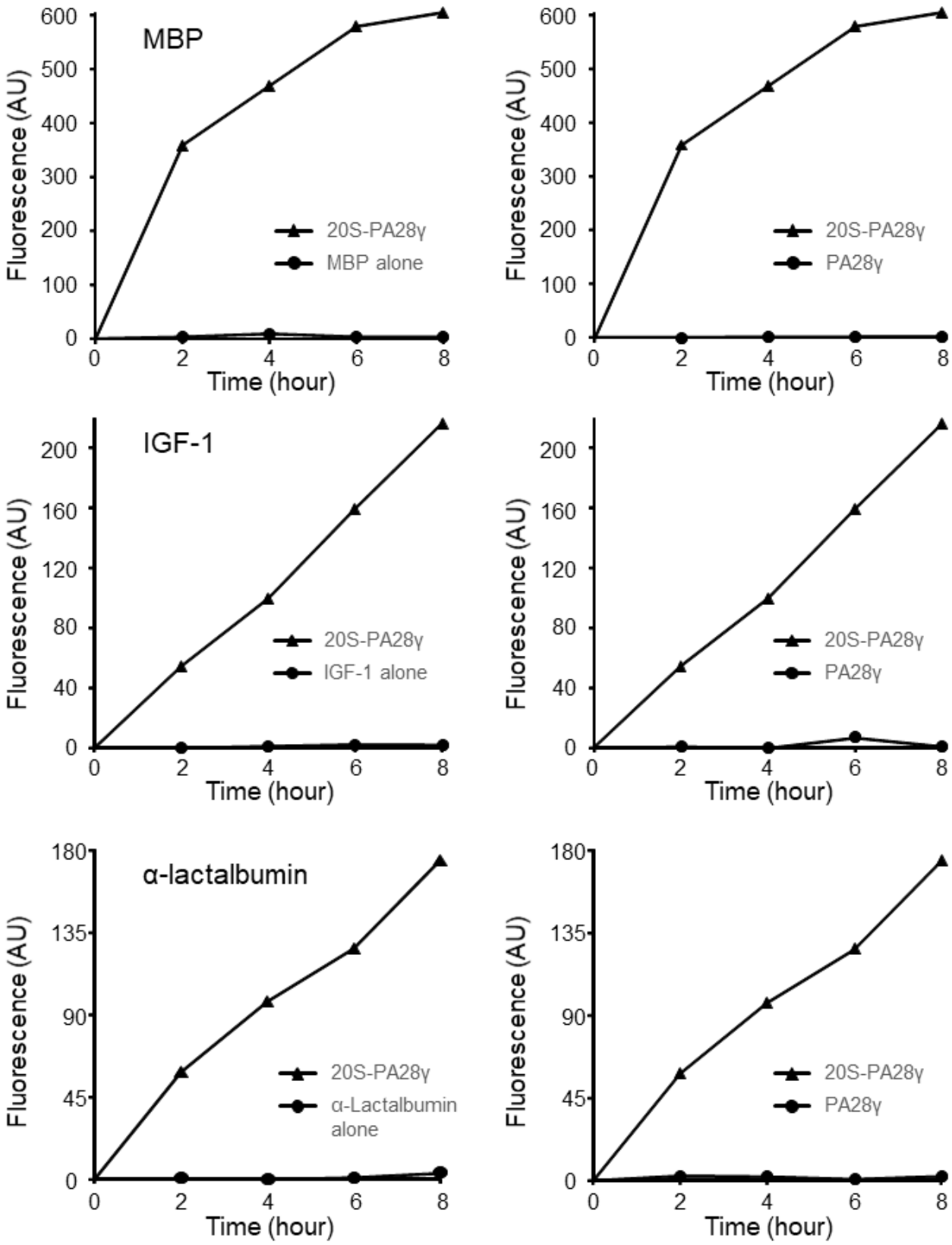

Supplementary Fig. 6

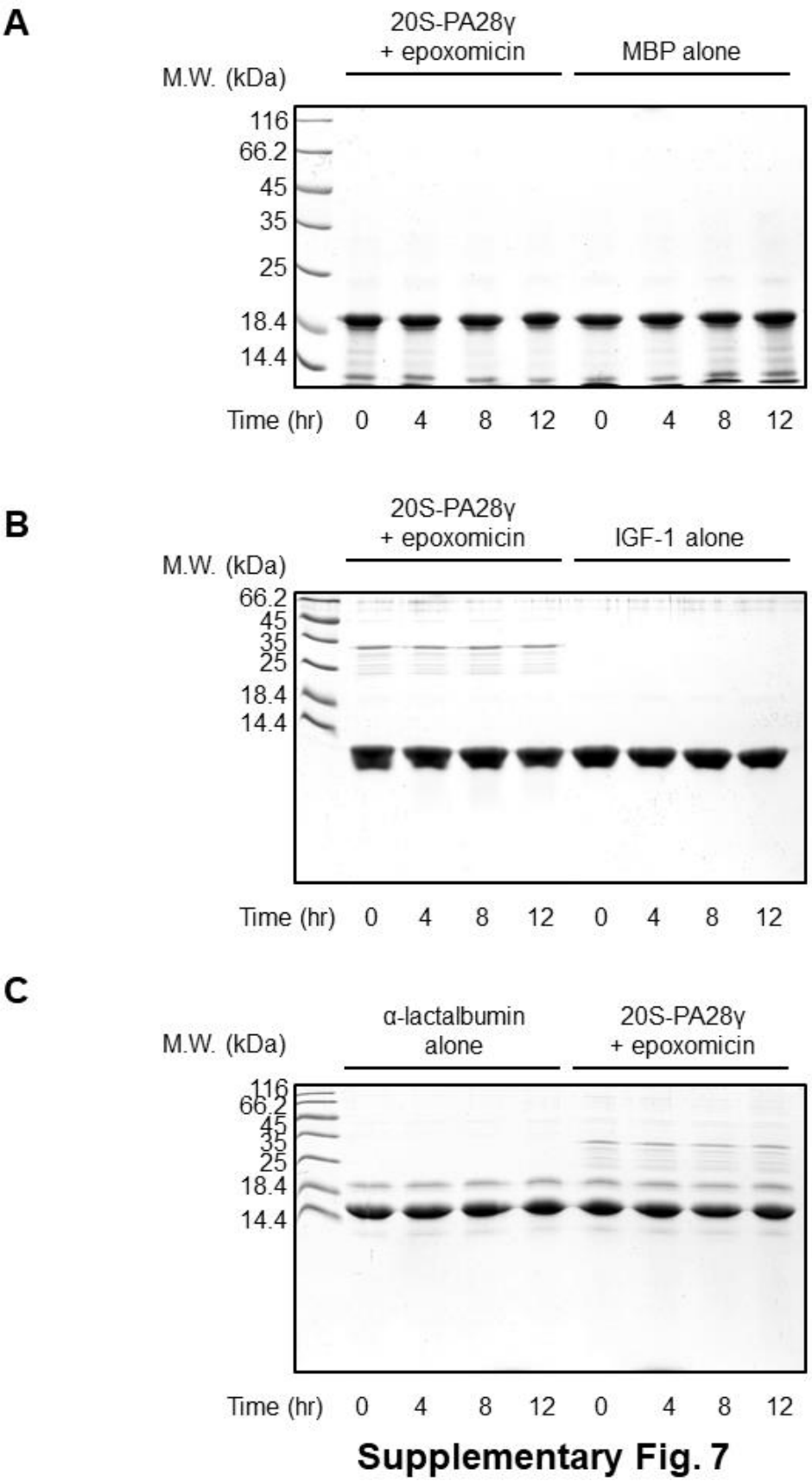

Supplementary Fig. 7

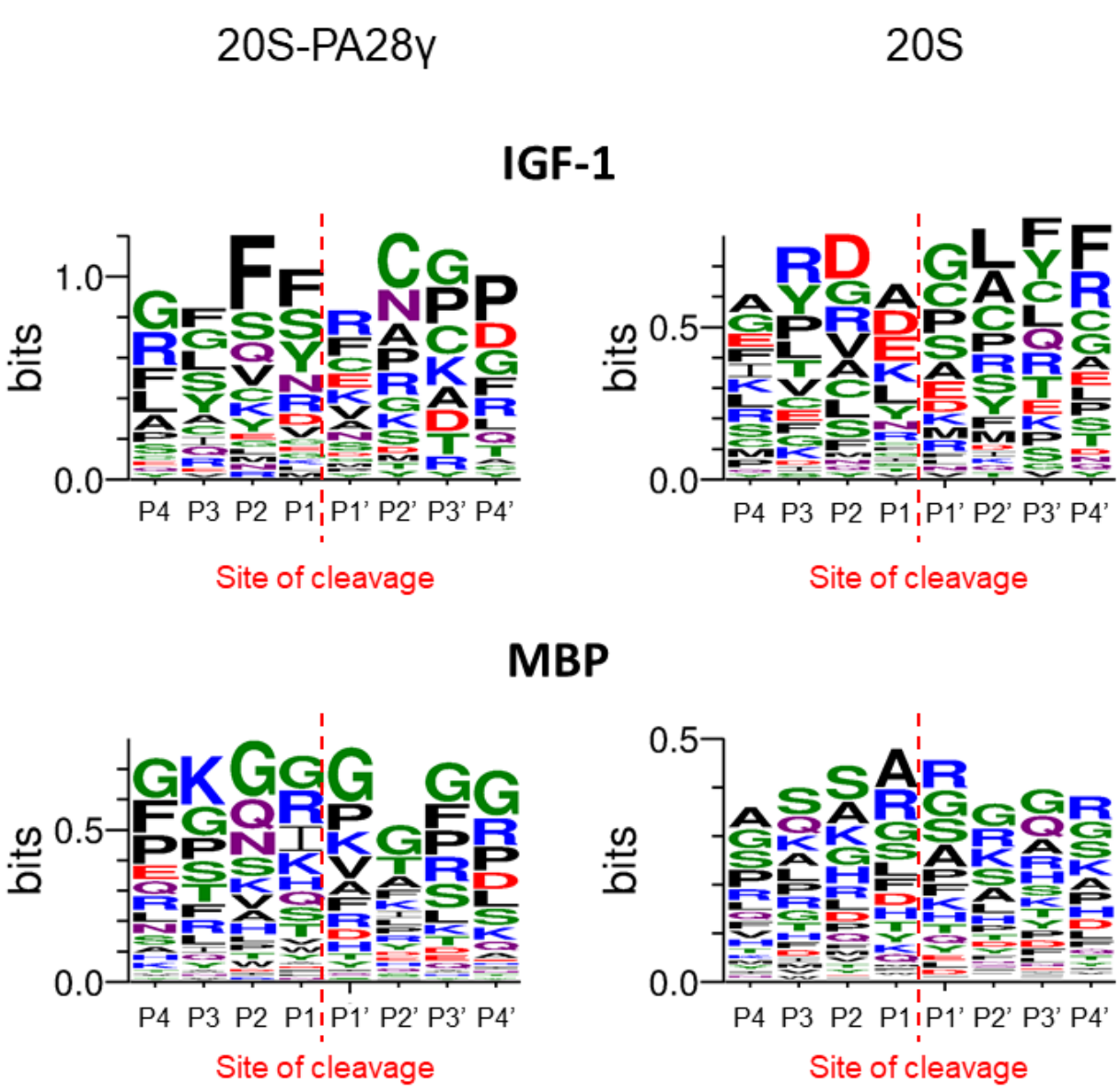

Supplementary Fig. 8

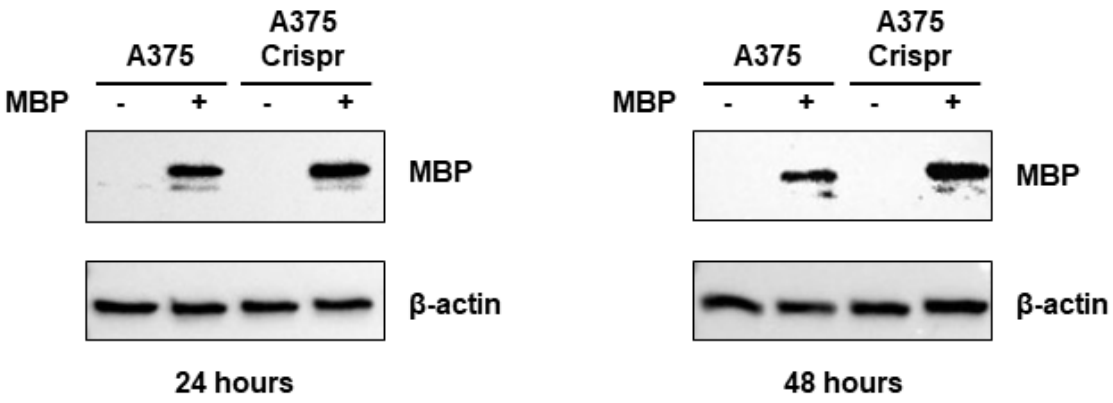

Supplementary Fig. 9

Proteasomal activity	Substrate	20S specific activity (nmol peptide cleaved /mg 20S * min) ± SE	+ Epoxomicin
Chymotrypsin-like	Suc-LLVY-amc	12,27 ± 0,76	0
	Suc-LY-amc	16,29 ± 1,43	0
	Suc-GGL-amc	95,90 ± 2,62	0
	Suc-AAF-amc	40,10 ± 0,79	0
Caspase-like	Suc-YVAD-amc	3,76 ± 0,53	0
	Suc-DEVD-amc	1,05 ± 0,04	0
Trypsin-like	Z-FR-amc	0,69 ± 0,03	0
	Z-LR-amc	0,64 ± 0,03	0
	Z-RR-amc	0,36 ± 0,02	0
	Bz-VGR-amc	60,94 ± 3,23	0
	Z-ARR-amc	33,93 ± 1,50	0
	Boc-LRR-amc	24,97 ± 0,79	0

Supplementary Table 1 20S proteasome specific activities. 20S proteasome specific activities were assessed as described in the Materials and Methods with a panel of fluorogenic peptides to probe each proteasomal cleavage specificity. Data are the means of three to five independent measurements ± SEM.